Final Technical Report
COVER PAGE

Federal Agency to which Report is submitted: DOE EERE – Wind & Water Power Program

Recipient: Florida Atlantic University, DUNS Number: 004147534
Award Number: DE-EE0006386
Project Title: Effects of EMF Emissions from Cables and Junction Boxes on Marine Species
Project Period: Start Date: Jan 1, 2014 to June 30, 2016

Principle Investigator:
Dr. Manhar Dhanak, Professor & Director, email: dhanak@fau.edu; Phone: 954 924 7242
Report Submitted by: PI

Date of Report: 09/29/2016
Covering Period: Jan 1, 2014 to June 30, 2016

Working Partners:
1) Nova Southeastern University. Co-PI: Prof. Richard Spieler; spielerr@nova.edu; V: (954) 262 3613
2) NSWC-CD. POC: Dr. Bill Venezia, Chief Engineer; william.venezia@navy.mil; V: (954) 926 4001

Cost-Sharing
Partners: Florida Atlantic University and Nova Southeastern University

DOE Project Team: DOE HQ Program Manager – Alejandro Moreno
DOE Field Contract Officer – Laura Merrick
DOE Field Grants Management Specialist – Jane Sanders
DOE Field Project Officer – Gary Nowakowski
DOE/CNJV Project Monitor – Nicholas Massey

Report Authors: Manhar Dhanak[*], Richard Spieler[+], Kirk Kilfoyle[+],Robert F. Jermain[+], John Frankenfield[*], Shirley Ravenna[*], Christopher Dibiasio[*], Robert Coulson[*], Ed Henderson[*]
[*]Florida Atlantic University
[+] Nova Southeastern University

Acknowledgment: "This material is based upon work supported by the Department of Energy and the Bureau of Ocean Energy Management under Award Number DE-EE0006386."

I. EXECUTIVE SUMMARY

Studies have shown that diverse aquatic species are electrosensitive. Many fishes, and marine mammals, can either detect, navigate by, or are affected by electromagnetic fields (EMF) with various sensitivities, and their behavior may be impacted by unnatural EMF emissions in the water column. Sharks, rays and skates are known to have the highest sensitivity to electric fields. Electric field emissions in the range 0.5–100 micro volt/m appear to attract them, and emissions over 100 micro volt/m to repulse them. A marine hydrokinetic MHK device will have multiple components and associated multiple submarine cables on the seafloor and running through the water column and would potentially increase the level of EMF emissions to which the marine species at the site may be exposed to. There are therefore concerns amongst stakeholders that EMF emissions associated with MHK devices and their components may act as barriers to species migration, cause disorientation, change community compositions and ecosystems, and that they may attract sharks, leading to a local increase in the risk of shark attacks. However, field data to validate and model potential relationships between observed responses and the EMF emissions *in situ* are sparse.

A program of experimental field surveys were conducted off the coast of South Florida, USA to characterize the electromagnetic field (EMF) emissions in the water column from a submarine cable, and to monitor for responses of local aquatic species. The field surveys were conducted at the South Florida Ocean Measurement Facility (SFOMF) off Fort Lauderdale, which is a cabled offshore in-water navy range. It consists of multiple active submarine power cables and a number of junction boxes, with the capability to transmit AC/DC power at a range of strength and frequencies. The site includes significant marine life activities and community structure, including highly mobile species, such as sharks, stingrays, mammals and turtles. SFOMF therefore typifies a setting representative of an offshore location where a MHK device may be sited.

Background electromagnetic field (EMF) levels and EMF emissions due to submarine cables were measured using a custom E-field sensor and a commercial magnetometer deployed from an autonomous underwater vehicle (AUV) at various fixed altitudes above the seafloor. EMF signatures detected from power cables and junction boxes are contrasted against ambient background levels and other EMF sources. The potential responses of local marine species were observed at selected representative locations using divers on SCUBA, complemented with fixed cameras on the sea bottom and by a set of video cameras mounted on the AUV. The objectives of the study were: 1) to characterize the EMF emission levels associated with submarine cables 2) to monitor potential responses of aquatic animals to the emissions and 3) to develop an associated database of field observations. As control, observations of EMF levels and *in situ* marine species were conducted with power in the cable turned off.

Good quality measurements of EMF emissions were obtained using the mobile AUV platform and the data from the surveys were used to develop contour maps of the EMF levels in the water column above the live cable as well as to provide information about how the field decays away from the cable. The measurements show good agreement with

theoretical models of the how EMF levels decay away from the cable in deep and shallow water environment. Electric fields in excess of 200μV/m were measured in the vicinity of the cable during the power on state.

Quarterly surveys by SCUBA divers were conducted, using point and transect count methods, over a period of one year at three locations, one at a shallow site where the water depth is approximately 5m, and the other at the Barracuda Reef where the water depth is approximately 10m. The sampling results were analyzed to determine if the presence of an SFOMF generated EMF alters: (1) abundance, species richness, and assemblage structure of coral reef fishes, (2) the behavior of fishes including elasmobranchs, and (3) the distribution of marine turtles and mammals. Diver observations were also used in attempt to discern if there were any noticeable organismal responses during the transitional period between ambient OFF to energized AC or DC power states, and video footage was intended to augment the *in-situ* visual survey data and aid in interpretation of the results. Comparisons are provided between observation datasets between the three sites and between the point and transect count methods. Presence of several individual elasmobranch species, including sharks and stingrays, were recorded during the surveys. No apparent effect on richness could be discerned between the power on and off states. No apparent sudden animal movements were observed during transitions between power states.

II. INTRODUCTION

Studies by Fisher and Slater (2010) and others (Gill and Taylor, 2002; CMACS, 2003; Tricas and Gill, 2011) have shown that diverse aquatic species are electrosensitive or magneto-sensitive. Many fishes and other animals can detect electric fields with various sensitivities and use them for prey detection, finding mates, and perhaps orientation. Some fishes, cetaceans, turtles and other animals sense the magnetic field and use it for orientation and navigation during extensive migrations and for homing. Sharks, rays and skates are known to have the highest sensitivity to electric fields, with sensitivities in the range 0.5–1000 $\mu V/m$, although some elasmobranch species have sensitivities as low as 1 nV/m. Electric field emissions in the range 0.5–100 $\mu V/m$ appear to attract some species, and those over 100 $\mu V/m$ repulse them (Gill and Taylor, 2002, Tricas and Gill, 2011). There is significant lack of research into the potential impacts of EMF on sea turtles and marine mammals. Kirschvink et al. (1986) suggest that the guiding 'map' sense of migratory cetaceans may be largely based on a simple strategy of following paths of local magnetic minima and avoiding magnetic gradients. Klimley et al. (2002) suggest that white sharks use magnetic lineation in moving through the water column. Westerberg and Lagenfelt (2008) observed that European eels slowed down in their movement when crossing cables carrying AC power. Therefore, the behavior of these organisms may be impacted by unnatural EMF emissions in the water column.

There are concerns amongst permitting agencies and stakeholders regarding the potential effects of EMF emissions associated with offshore energy conversion (OEC) devices and their components on marine organisms (Fisher and Slater, 2010). Typically, OEC will involve multiple devices and associated multiple submarine cables on the seafloor and running through the water column, potentially subjecting marine species to significant levels of EMF emissions. Concerns with such EMF emissions include that they may attract/repel sensitive species, act as barriers to movement and migration, cause disorientation, and change community compositions and ecosystems, although the evidence for any of these concerns

is sparse. EMF emissions from submerged cables depend on transmitted power, whether the power supply is AC or DC, the frequency and amplitude of the AC current, and cable construction (CMAS, 2003). Their characteristics also depend on whether seawater ground or two-wire ground is used and whether the cable is buried, on the seabed, or suspended in the water column; the effect of cable burial will be through reduction in the distance to the surface of the cable, although it will not significantly reduce the magnetic field in the water column since the relative permeability of the seawater and the seabed are both approximately uniform. EMF emission levels from a power carrying cable decays inversely with distance from it. The electric field depends on the potential across the cable and increases with it while the magnetic field depends on the flow of current through the cable and increases with the magnitude of the current. A COWRIE report (CMAS, 2003) concluded that there is lack of consensus on the characteristics of the EMF emitted by subsea power cables to enable making an informed assessment of any possible environmental impact of EMF emissions in the range of values likely to be detected by organisms sensitive to electric and magnetic fields. There is a clear need for field data on EMF emissions from submarine cables in order to develop realistic EMF propagation models, based on Maxwell's equations, for predicting such emissions (see for example, CMAS, 2003). Models, based on field observations and laboratory experiments, are also needed for predicting the impact of EMF emissions on marine organisms such as significant changes in population or ecological communities.

The US Navy's South Florida Ocean Measurement Facility (SFOMF) off Fort Lauderdale is a cabled in-water range that consists of a number of active submarine power cables and junction boxes Venezia et al. (2003). The cables have a range of capabilities for power supply, including DC and AC power of various frequencies and amplitudes. SFOMF therefore provides a suitable setting to examine EMF emissions and their effects on local aquatic species. Emphasis was on examining responses of electro-sensitive species in the region. EMF levels at selected representative locations along a submarine cable were measured using a custom E-field sensor and a commercial magnetometer deployed from an autonomous underwater vehicle (AUV).

The southeastern continental shelf and shelf edge off Florida supports diverse and recreationally and economically important reef-fish communities (Ferro et al., 2005; Bryan et al., 2013). There is rich literature on the geology and biology associated with the shelf and the surrounding area that has documented an abundant and diverse marine community, including teleost fishes, elasmobranchs and turtles (Baron et al., 2004; Spieler et al, 2013). Multiple species of electrosensitive sharks and rays reside in the area and/or migrate through on the way to or from breeding sites (Castro, 1994; Schwartz ,1990). For example, the yellow stingray, *Urobatis jamaicensis*, is very abundant in the area (Spieler et al, 2013). The electro-sensitive abilities of sharks and rays are used for multiple species-dependent functions such as feeding, predator avoidance, reproduction, and orientation Helfman et al. (2009). Thus, disruption of electro reception could potentially have significant consequences for these animals.

The South Florida region has a significant potential for ocean energy resources associated with the Florida Current (see for example, Duerr and Dhanak, 2012) and is of high interest to OEC developers seeking to develop technologies in harnessing the energy of the Florida Current. The proposed study therefore has an added significance.

III. OBJECTIVES

The primary objective of the effort was to measure and characterize EMF emissions in the field and conduct in-water monitoring to assess behavioral and benthic community effects of EMF emitted from submarine cables, junction boxes and other related sources, as representative of significant components of MHK devices, with an emphasis on local aquatic species. The specific objectives were:

- To characterize, through temporal and spatial measurement, background EMF levels and EMF emissions in a region from submarine cables, identifying EMF signatures associated with these components.
- To monitor and study potential effects of these EMF emissions on aquatic species with the aim of determining whether the EMF field attracts/repels them, serves as a barrier to their movement and migration, and introduces changes in benthic community composition, abundance, and size structure.
- To develop a database for field measurement of EMF emissions associated with submarine cables and related components and associated organismal responses.
- To determine, using the field measurements of EMF emissions and organismal response data, the relationship between potential observed changes and the EMF emissions and to assess the potential ecological impact (if any) of EMF on individual organisms, populations, and species in the vicinity.

IV. APPROACH

The objectives of the work were 1) to characterize, through temporal and spatial measurement, background EMF levels and EMF emissions from submarine cables and other related EMF sources in the region, 2) to monitor for potential responses of local aquatic species to elevated EMF levels at the site, and 3) to develop a database of EMF levels and organismal responses to support assessment of the potential ecological impact (if any) of EMF on the aquatic animals. The aim was to identify procedures that can be utilized at any OEC site.

In order to assess temporal and spatial variability, three representative subareas (Fig.1) on the SFOMF range were selected, referred to as the inner-reef (5m depth, 0.6km from shore), middle-reef (10m depth, 1.4km from shore) and outer reef (15m depth, 2.4km from shore). The subareas are approximately 1 km apart and were carefully selected based on characteristic depth zones and habitat types (two factors known to influence the composition of local fish assemblages), previous surveys of organismal activities, and distribution of cables and associated power components. Previous studies suggest strong seasonal patterns in animal occurrence in near shore waters, so that quarterly surveys are appropriate.

Fig. 1:SFOMF site in South Florida (left), and the inner (shallow), middle (Barracuda), and the outer (deep) reef sampling subareas at the SFOMF site offshore of Port Everglades (right).

A. Surveys of EMF levels

A custom electric-field sensor and a SeaSPY Marine Magnetics magnetometer were deployed from an AUV to characterize it for EMF levels Dhanak et al. 2013; Dhanak et al., 2015). The magnetometer is towed from the vehicle 10m behind the vehicle and 1.8m beneath the AUV, while a custom 3-axes electric field sensor is mounted on the AUV (Fig. 2); the implementation of these sensors onto the AUV is described in (Dhanak et al., 2015). The E-field sensors were calibrated in the laboratory and validated in the field using a known source.

AUVs are suitable mobile sensor platforms for in-water surveys (Dhanak et al., 1999; An et al., 2001). A Bluefin 21 AUV, which is approximately 3m long and has a 0.53m maximum diameter, is used for the surveys. The AUV has a `modular' design, with a fixed set of motor, batteries, navigation instruments, controls and the main central processor unit located in the rear half of the submarine, but with a custom designed front section, of 1-2m length, for the pay-load. The vehicle has a cruising speed of 1.5 m/s. It records six-degrees-of-freedom motion using an inertial navigation-grade motion sensor, coupled with a GPS and a Doppler velocity log (DVL) with bottom-tracking lock, to navigate. The AUV is equipped with upward (600kHz) and downward (300kHz) looking acoustic Doppler current profilers (ADCPs) and a conductivity-temperature-depth (CTD) measurement system. The latter measures *in-situ* conductivity and temperature in the water column. The AUV is programmed by setting navigational waypoints, speed, altitude and other parameters. It records its position at the surface via its GPS unit and dives to the desired altitude where it navigates by dead reckoning, reporting its inferred position at constant intervals to the surface ship via an acoustic modem. The positional information is recorded, together with the water depth, altitude, and measurements from other sensors to provide geographic reference to the measurements.

Fig. 2: Schematics of the towing of the SeaSPY magnetometer

B. *Monitoring surveys of organismal response activity*

Marine life activities at the three selected SFOMF subareas in the vicinity of the cable were monitored during the experiments by divers on SCUBA, an AUV equipped with high-resolution video cameras, and by bottom-mounted video stations. The procedure allowed for providing complementary observations based on the different methods. Organismal response surveys were conducted with the power in the cable on (DC and AC, separately) and off; the latter serving as a control condition.

1) SCUBA diver-based surveys

SCUBA-based surveys use two standardized methods, stationary point count and transect-line count (Figs. 3 and 4), to record fish species, size, and abundance. In the stationary point count, all the fish are counted in an imaginary cylinder, 15 m in diameter, from the substrate to the water surface. For the first five minutes, only the species are recorded. After the five-minute species-count is completed, the number of fish per species and the minimum, maximum, and mean fork length of each species are recorded. The diver accomplishes the count by staying in the center of the cylinder and rotating 360° to record species and length. For the transect-line, a 30-m line is deployed along the cable. The diver swims above the transect, recording all fish within 1 m of either side and 1 m above the line (an imaginary 60m^3 tunnel). Abundances and fork length (FL) (by size class: <2, 2-5, 5-10, 10-20, 20-30, 30-50 and 50+ cm) of fish species are recorded. In both types of counts, the diver carries a 1-m ‘‘T’’-rod, with the size classes marked off, to aid in fish length and transect width estimation. These statistically validated survey methods provide data amenable to rigorous statistical analysis [9, 11, 24]. A one-way analysis of variance, ANOVA, between means is a primary analysis. In addition, potential differences in fish-assemblage structure and similarity percentages among sites are examined using the Bray-Curtis dissimilarity index with multidimensional scaling (MDS) ordination and SIMPER [11, 24].

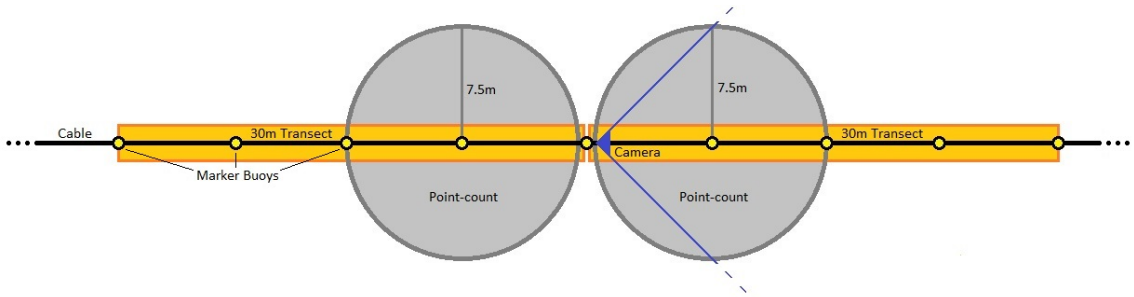

Fig 3: Schematic of the fish count layout used at each site. The blue lines illustrate the camera’s field of view.

2) AUV-based surveys

The AUV autonomously follows the terrain 3-4 m above the seafloor, collecting high-resolution color imagery within the water column while maintaining a forward speed of 1.5m/s. Lawn-mower pattern path surveys are conducted over the region in the vicinity of the cable including the 15m-circlular point-count station mid-way along the path. The AUV carries two 12 megapixel, low-light GoPro cameras, one mounted on the AUV hull, and the other located on the towed magnetometer (Fig. 5). The imagery from the cameras is analyzed to characterize activities in the local reef fish communities and identify species. The video is time-stamped and, in conjunction with the navigation data from the AUV, provides geographic position reference to each video frame.

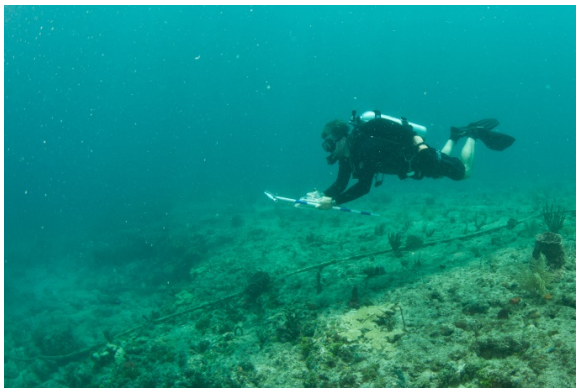

Fig. 4a: A diver conducting a transect survey along the cable at the middle-reef site in the vicinity of the cable.

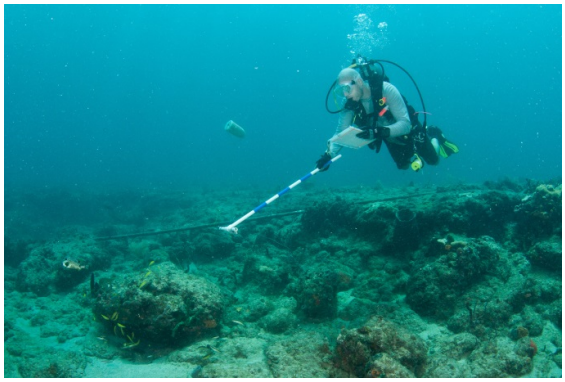

Fig. 4b: Diver conducting a point-count survey.

Fig. 5: Video cameras are flush-mounted on the underside of the AUV hull and on the magnetometer.

3) Bottom-mounted underwater video stations

Three bottom-mounted underwater video stations were established, one at each subarea at the site to determine the differences in organismal response between when the power in the submarine cable is on and when it is off. A high-resolution GoPro camera was mounted on a tripod at each location (Fig. 6). These stationary video cameras provide fixed views in the vicinity of the cable. Cameras on tripods are set up on the seafloor at each site by divers prior to the SCUBA surveys to collect simultaneous fixed camera observations to compliment the SCUBA surveys. For each camera, organisms in the entire field of view were recorded for the power ON and power OFF sequences, including transitions between the two. The video cameras also capture activities in the vicinity of the cable in the absence of the divers. The videos from these stationary sites are analyzed in a way that will be amenable to rigorous statistical analysis, as follows: For each power ON or OFF sequence, the video is reviewed and minute-long counts are conducted in which the total number of fish species observed is tallied. This was done multiple times during each sequence to generate a mean abundance value for each power sequence. Repeating the process for each power sequence allows for calculation of standard errors and performance of statistical tests on the results. In addition to total abundance estimates, qualitative data on animal movement and behavior were obtained by reviewing the video at the exact moment of power transition and during each power sequence to gauge any startle or other overt responses. The stationary videos are analyzed in terms of species-specific abundance, including prevalence of any species during power ON state as well as orientation and qualitatively, the movement of the animals during changes in power states. For sharks and rays, in view of the relatively low level of EMF emissions, we expect the movement to be toward the cable when the power is switched on. For other fish, the response needs to be determined.

Fig. 6: Bottom-mounted camera on a tripod.

V. EMF Level Characterization

A. AUV-based measurement system

Autonomous underwater vehicles (AUV) are suitable tether-free mobile sensor platforms for in-water surveys and have been demonstrated to provide good quality measurement of various physical variables (see for example An et al., 2001, Dhanak and Holappa, 1999).

To measure and characterize the subsurface magnetic field, a SeaSPY magnetometer by Marine Magnetics Corporation is towed from a Bluefin 21 AUV through the water column by a 10m cable as schematically shown in Fig. 2 Venezia et al. (2003). The SeaSPY is an Overhauser magnetometer that measures the total magnetic field with a sensitivity of 0.01nT and resolution of 0.001nT at a sampling rate of 1-4 Hz. The SeaSPY also includes a depth sensor and operates at very low power levels, while maintaining its high sensitivity. The unit is powered via the tow cable by the AUV batteries. The sensors onboard the AUV include an upward (600kHz) and a downward (300kHz) looking ADCPs, a CTD package, a depth sensor and an Inertial Measurement Unit (IMU).

Electric field measurement in seawater is achieved through the use of two electrical points in contact with the seawater that are connected to a voltage-measuring device. The straight line between the two contacts gives the direction of the E-field. The measured voltage divided by the separation distance between the contact points gives the electric field, expressed in volts per meter. The contact points, or electrodes, are designed in such a way that they produce minimal voltage in the absence a source of electric field. The voltage measured by a two-electrode sensor depends on the electrode spacing. Three pairs of electrodes are orthogonally configured to provide a 3-axes E-field sensor. The sensing element is silver (Ag) which forms silver chloride (AgCl)) in seawater. It is non-polarizable and as such has relatively constant potential in response to small changes in current. Ag/AgCl sensors are robust and have excellent long-term stability [9.10].

The electrodes have a low contact resistance with the seawater, resulting in low noise levels Venezia et al. (2003). Each is enclosed in a cup-like housing, filled with a saltwater agar bridge (Fig 7). Contact with the seawater is via this porous barrier, which minimizes contaminants from entering the chamber, shielding the electrode and helping to minimize biofouling. The housing also reduces the flow noise.

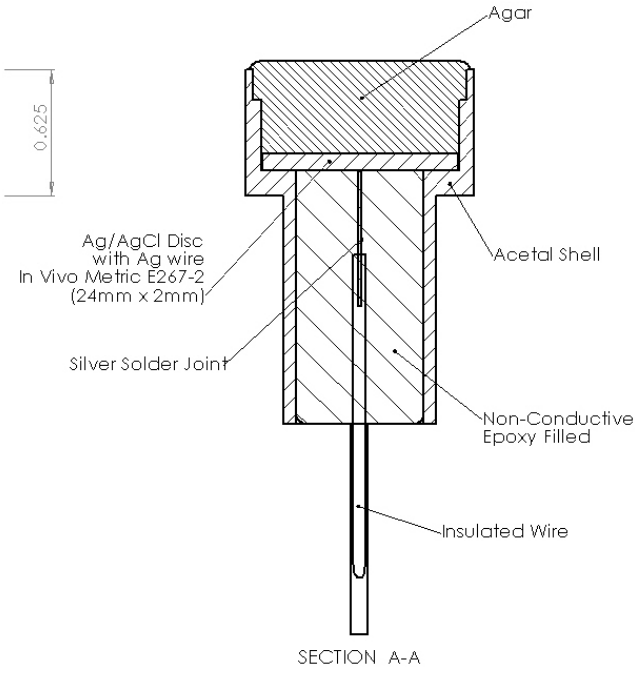

Fig. 7: Ag/AgCl Electrode

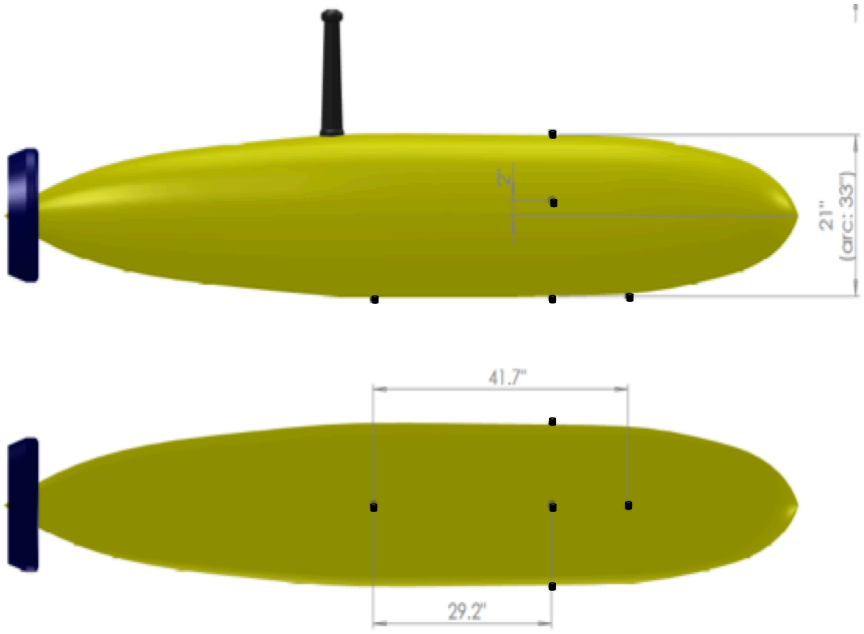

Fig. 8: Location of the E-field electrodes (black appendages) on the AUV hull.

The six electrodes are located on the AUV hull as shown in Fig. 8 to provide 3-axes measurement of the E-field. To determine the local E-field, measured potentials across pairs of electrodes are amplified using a specially designed low-noise amplifier with a fixed gain of 1000 and then routed to a 3-channel simultaneously sampled A/D converter. The digitized data is stored for post-processing and a sub-sample of the data is also sent to the AUV for real-time monitoring. The electronics for data processing are located in a self-contained on-board pressure housing (Fig. 9). By combining the three axial components of the electric field, the total field vector can be computed regardless of the vehicle's orientation.

The sensors were extensively tested and calibrated in the laboratory for a range of fields produced by AC/DC sources through placing the sensors at known distances from the source and verifying the amplitude characteristics of the sensors. Fig. 10 shows laboratory tests of the electrodes. The probe responses were tested at various frequencies. Fig. 10b shows measurements recorded in the three channels for emissions from a 10Hz power source.

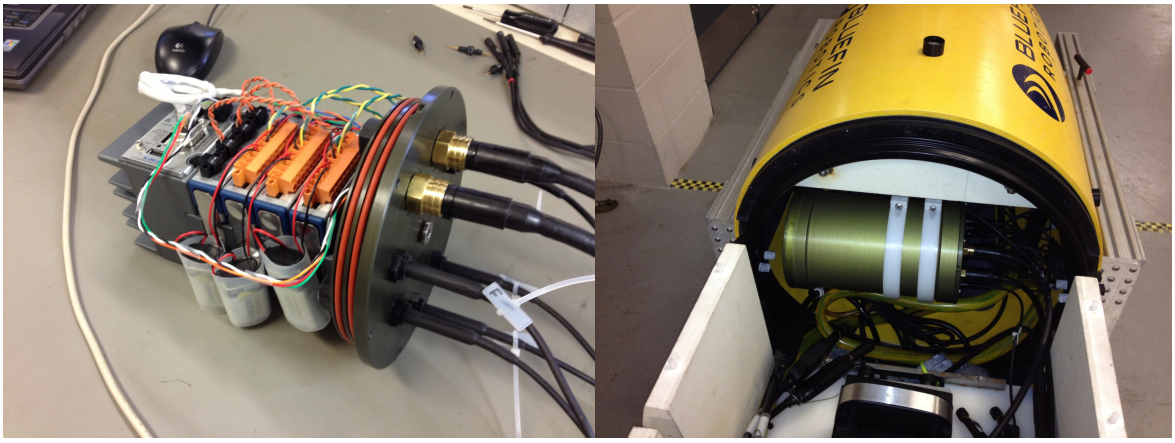

Fig. 9: E-Field processing unit and pressure vessel on board the AUV

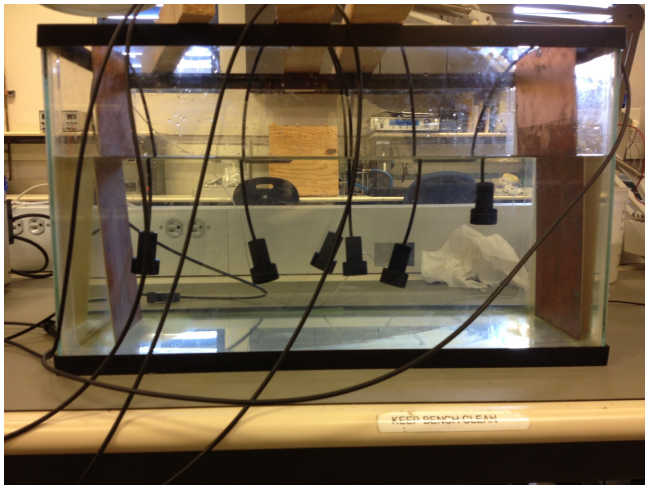

Fig. 10a: E-Field electrodes (three pairs) in test tank

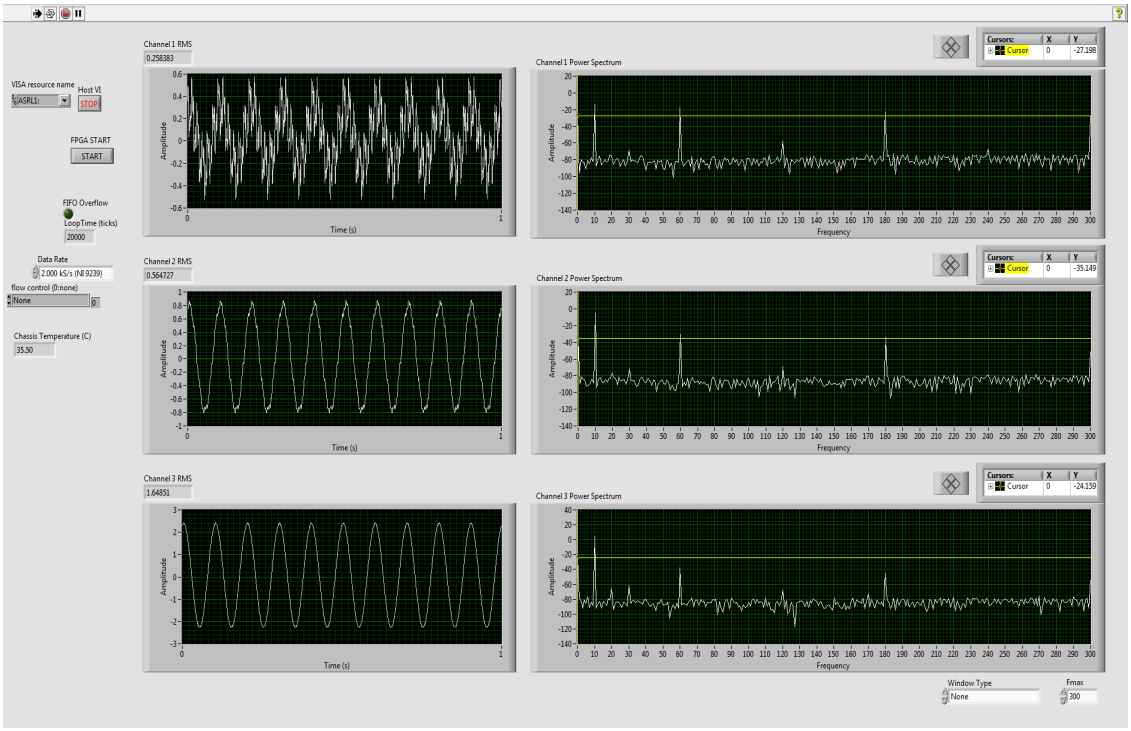

Fig. 10b. Measurement of emissions from a 10Hz test signal in lab test tank for all three channels.

The specifications for the cable are provided in Fig. 11. The mean *in-situ* conductivity (measured) of the seawater was $\sigma = 3.2\ s/m$. The relative permeability and the relative permittivity are estimated to be $\mu_r = 1, \text{and } \varepsilon_r = 74$ respectively. The power supply in the cables was varied to carry DC (0 Hz) or AC current at 60Hz; some initial runs were conducted at 5 and 10 Hz AC until it was determined at the Go-No-Go decision point that industry standard would be to use 60Hz AC for power transmission from MHK devices. The current amplitudes were in the range ~ 1 – 1.5 amps.

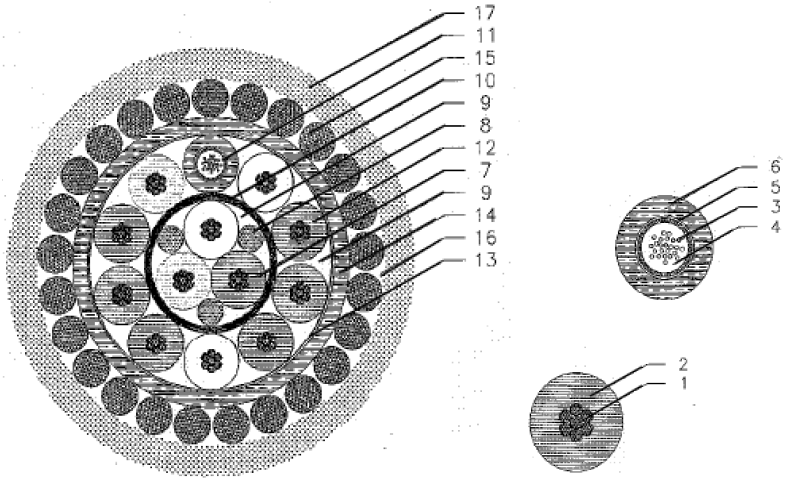

17		OUTER PROTECTION, PP-YARN	3.5	48
16		FILLING COMPUND, BITUMEN		
15	25	ARMOURING, GALV. STEEL WIRES	4.2	41
14		INNER SHEATH, POLYETHYLENE	2	32.5
13		WRAPPING, POLYESTER TAPE	0.05	28.5
12	9	UNIT-C. INSULATED CONDUCTOR, 4mm²	6.5	28.5
11	1	UNIT-FO, 24 off SM FIBERS	6.5	28.5
10		BEDDING, WRAPPING, PE-TAPE	0.75	15.5
9		FILLING COMPUND, PETROLEUM JELLY	.	
8	3	FILLER, POLYETHYLENE	3	14
7	3	UNIT-C, INSULATED CONDUCTOR, 4mm²	6.5	14
6		SHEATH, POLYETHYLENE	1.4	6.5
5		STEEL TUBE	0.25	3.7
4		FILLING COMPOUND		
3	24	SM FIBER		0.25
2		INSULATION, POLYETHYLENE	2	6.5
1		CONDUCTOR, Cu 4mm²	7X0.88	2.5
POS.	**QTY.**	**DESCRIPTION**	NOM. THICKN. mm	NOM. DIAM. mm

Fig. 11: Structure of the submarine cable (outer diameter 48mm)

B. Field Observations

A number of EM field-measurement missions were conducted at the deeper 3rd Reef site on the SFOMF range in the vicinity of the cable, with the power in the cable turned on/off. The water depth at the 3rd Reef is approximately 45m. The AUV was required to perform 'lawnmower pattern surveys' at various altitudes above the cable, with legs 100-200m long and 40-50m apart as desired, at a speed of 1.5 m/s. Measurement of the B-field using the towed magnetometer and the measurement of the E-field were carried out separately. Subsequent development now allows simultaneous measurement of both the E and B fields. Fig. 12a shows an aerial view of the AUV and the towed magnetometer, while Fig. 12b shows a view from a camera mounted onboard the towed magnetometer.

The AUV's lawn-mower pattern path across the cable, 4m above the bottom is shown in Fig. 13. The magnetometer, towed 10m behind and 1.8m below the AUV, provides observations of the B-field at an altitude of 2.2m above the seafloor. The legs of the path are approximately 100m long and 40m apart. The survey was carried out with the power in the cable off and then repeated with the power turned on.

Fig. 14 shows the time series of the B-field measured as the AUV traversed across the cable as indicated in Fig. 13 for the cases of DC power in the cable on and off. The measurements

include the background earth's magnetic field. As the sensor crosses the live cable, a peak in measurement of up to 150 nT is recorded. The characteristics of the signature as the cable is crossed depends on whether it is crossed from north to south or from south to north. This is because the measured total B-field includes the sum of the vertical component of the B-field emitted by the cable and that of the earth's magnetic field on one side of the cable, and a difference between the two on the other side. Fig. 15 shows the signature of the emitted B-field across the energized DC cable, obtained by subtracting the measured mean B-field during the survey. The field decays with distance from the cable, consistent with modeled B-fields (Gill and Taylor, 2002), as the AUV moves across the cable at 1.5 m/s

Fig. 12: AUV-towed magnetometer. (a) Aerial view, (b) View from the towed sensor

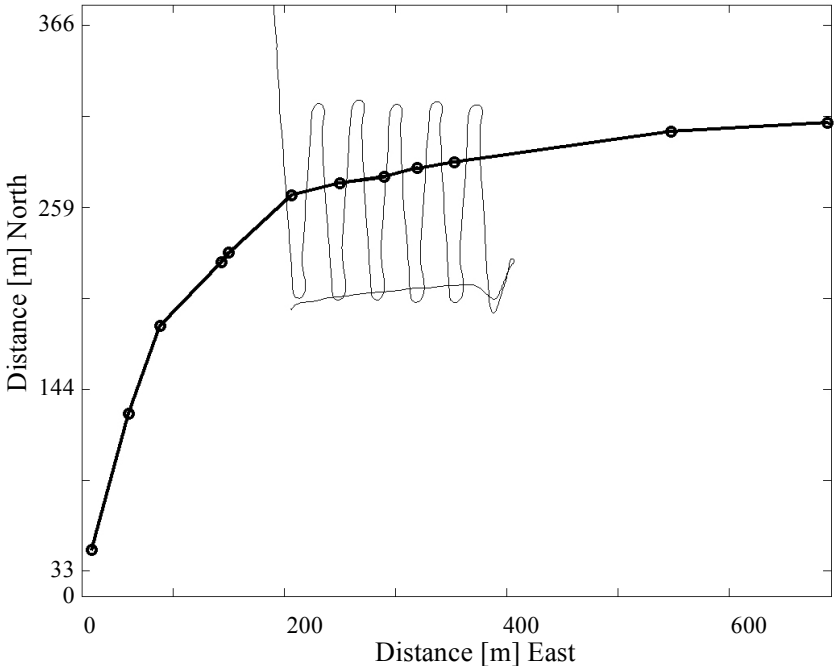

Fig. 13: Lawn-mower pattern survey path of the AUV at a depth of 4m across the expected location of the cable (thick black line)

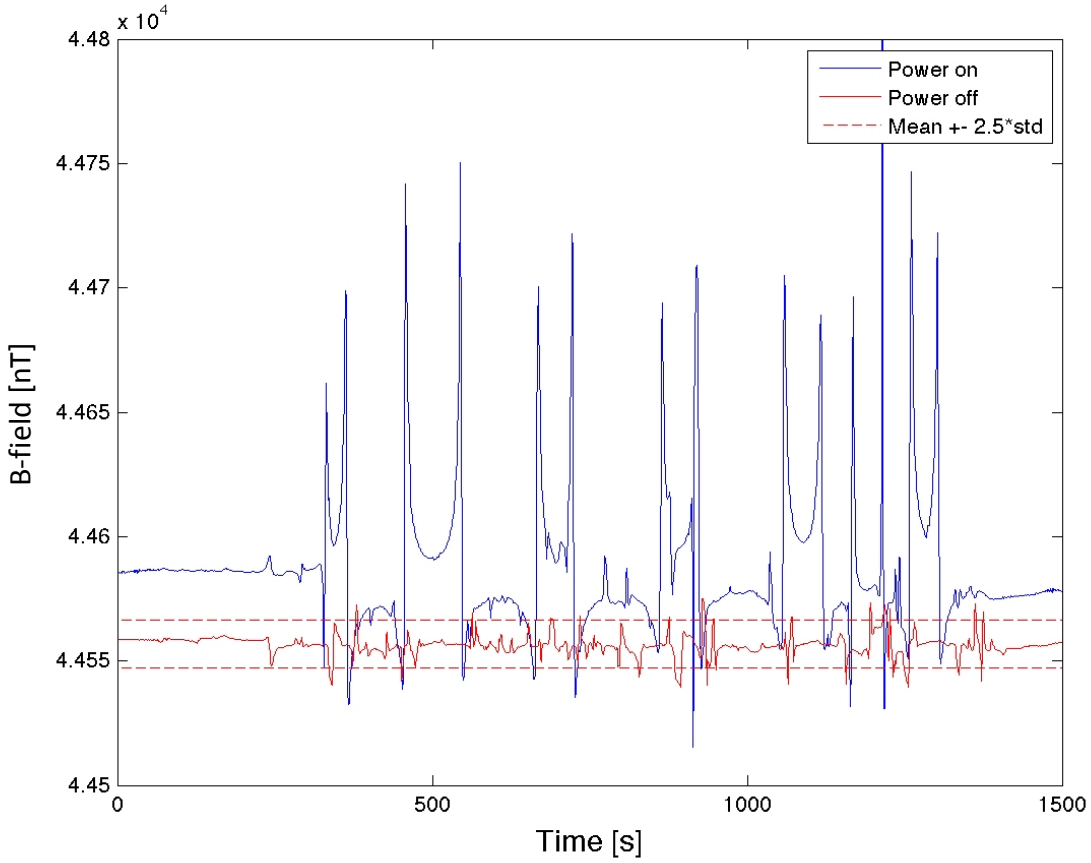

Fig. 14: B-field measured as the AUV traverses the path over the cable indicated in Fig. 13, for the power (DC) in the cable on and off. The dashed lines mark the ± 2.5 x standard deviation of the ambient field.

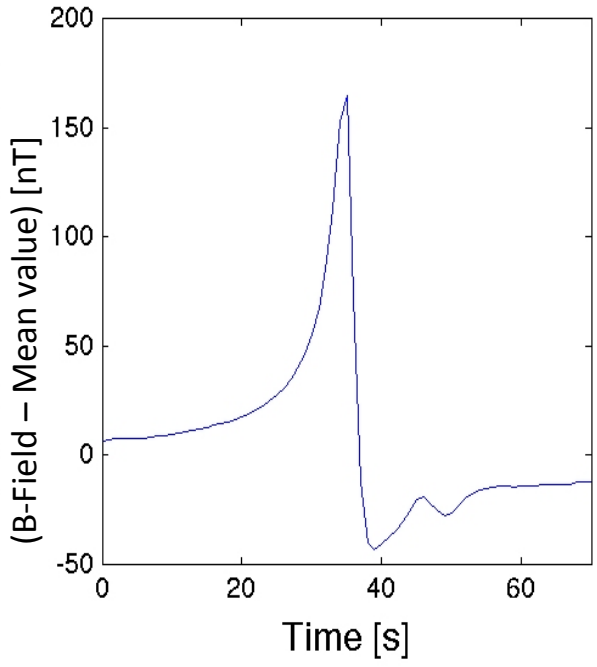

Fig. 15: Measured B-field signature during crossing of an energized DC cable

The measurements shown in Fig. 14 are utilized together with the position information recorded by the AUV to develop a contour map of the B-field over the region as shown in Fig. 16 for the case of the energized DC cable; the position of the sensor lags that of the AUV by 11s as it is towed behind the vehicle through the water. The contour map is developed through interpolation of the B-field recorded by the sensor as it is towed along the lawn-mower pattern path (shown superimposed in the figure). The mean B-field value at this altitude is approximately 30 nT above ambient, that is, when the power in the cable is turned off. Fig. 16b is the corresponding modeled magnetic field in the water column determined using the Biot-Savart law.

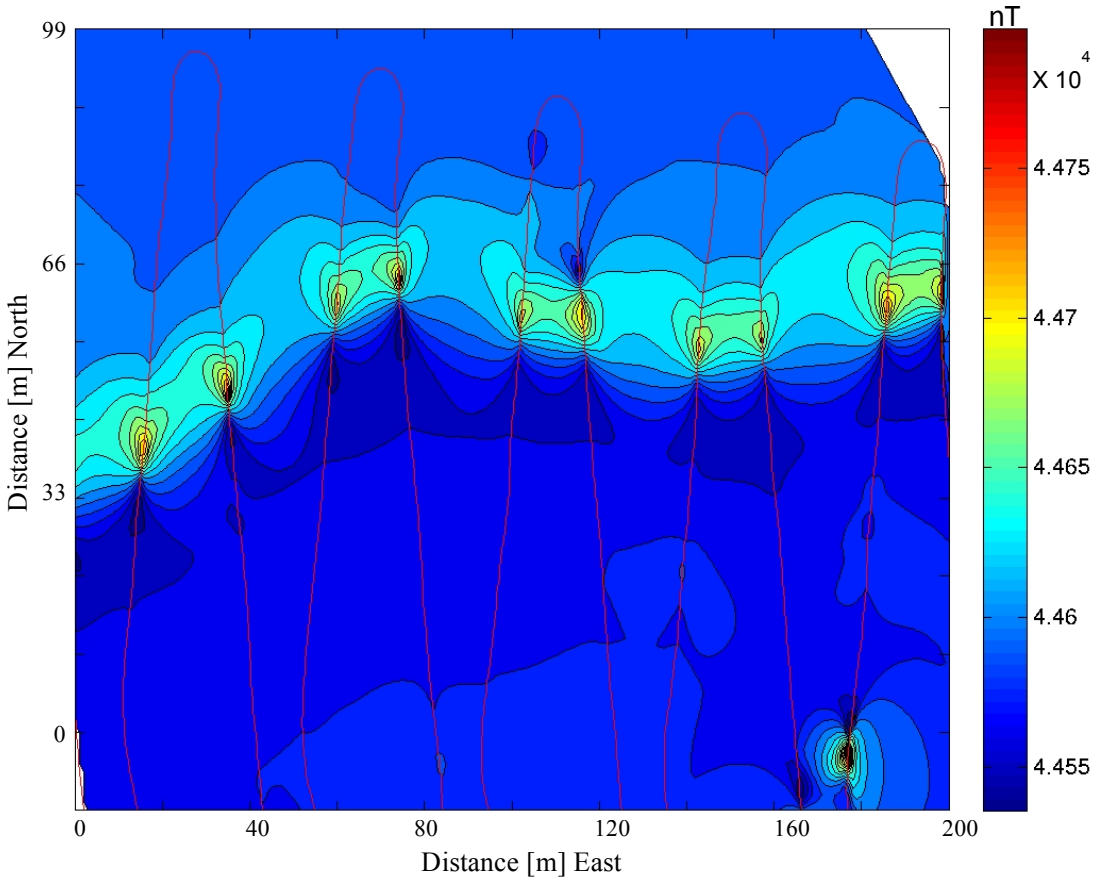

Fig. 16a: Characteristics of the B-field (nT) at 2.2m altitude above a submarine cable carrying DC power. The lawn-mower pattern path of the AUV is superimposed on the contour map.

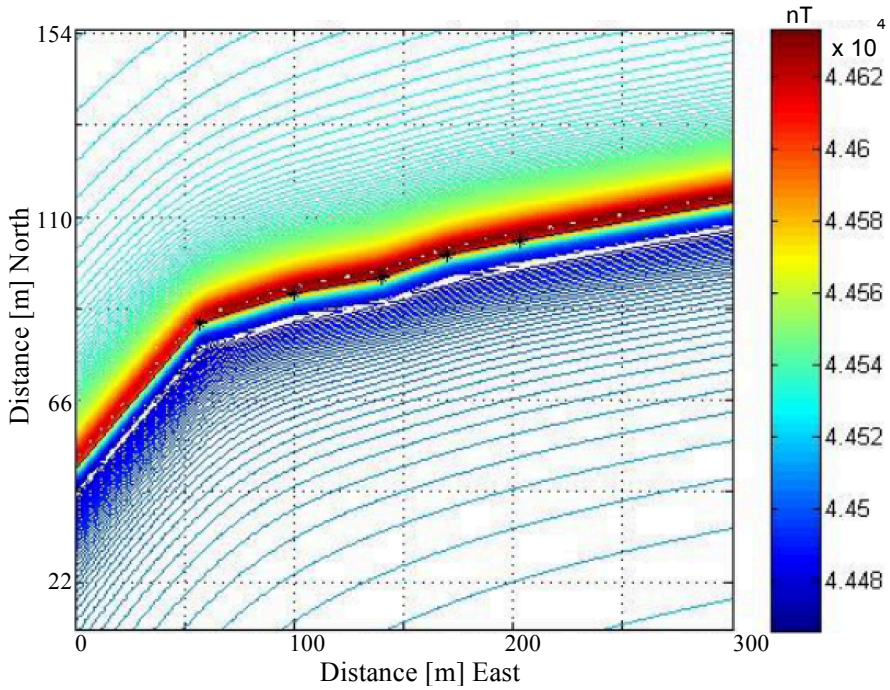

Fig. 16b: Modeled B-field (nT) corresponding to case in Fig. 16a.

No E-field was detected in the case of DC power as may be expected since the cable was shielded; slow motion of the AUV though the induced static B-field generates a low frequency E-field, but our sensors did not pick this up. A pair of surveys were conducted along the same path as shown in Fig. 13, but this time involving measurement of the E-field induced by an alternating B-field emitted from the submerged cable carrying a 10 Hz AC current and compared with the background field (with the power in the cable turned off). Fig. 17 shows the time-series of the root-mean-square of the measured E-field at an altitude of 4m above the seafloor in the cases with the power in the cable turned on and with it turned off. The background field has a mean value less than $10\mu V/$m. In comparison, the E-field emissions when the power is turned on reach values of up to over $60\mu V/$m 4m above the cable, the values peaking as the cable is crossed. Fig. 18 shows the signature of the emitted E-field across the energized AC cable, obtained by subtracting the measured mean field during the survey. It shows the expected decay of the induced E-field with distance away from the cable as the AUV once again traversed at a fixed altitude across the cable at 1.5 m/s.

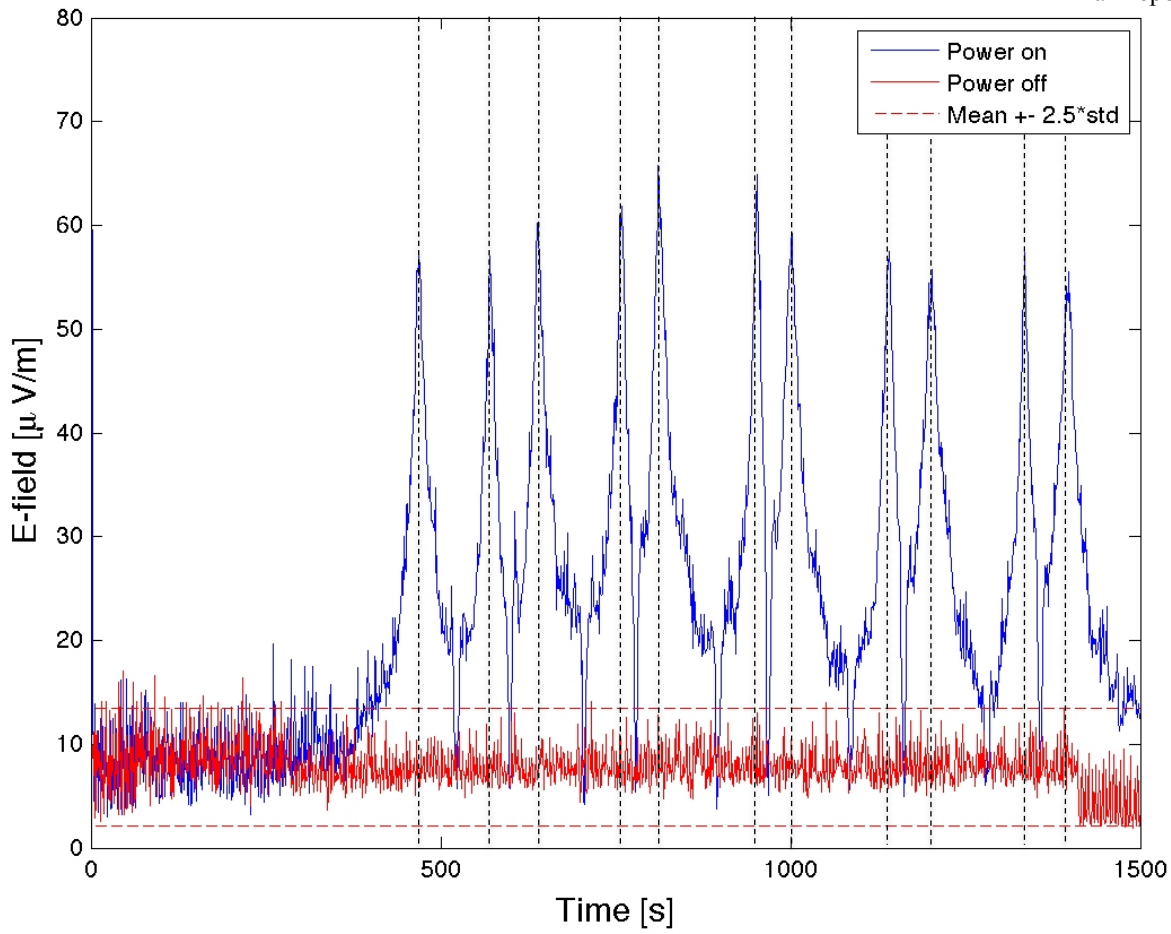

Fig. 17: RMS of the measured E-field as the AUV traversed at 4m altitude over the cable as indicated in Fig. 13 for the cases with 10Hz AC current in the cable turned on and off. Vertical dashed lines mark the times of cable crossing

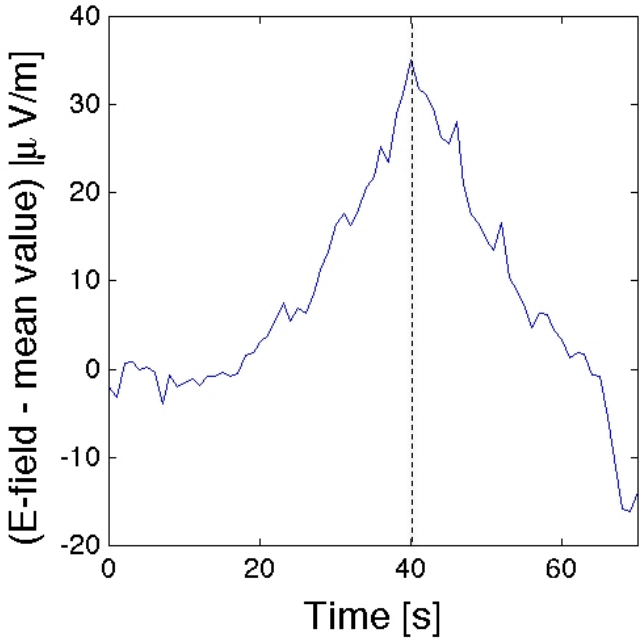

Fig. 18: RMS E-field signature during crossing of an energized 10Hz AC cable by the AUV travelling at 1.5 m/s. Vertical dashed lines mark the times of cable crossing

As in the case of the B-field, the measurements shown in Fig. 17 are utilized together with the position information recorded by the AUV to develop a contour map of the E-field over the region as shown in Fig. 19 for the case with the power in the cable turned on. Since the ambient E-field is small, the field over the surveyed region is dominated by the emissions from the cable (induced by the alternating B-field). The mean induced E-field value at this altitude is $22\mu V/m$ above ambient. The dashed lines mark the ± 2.5 x standard deviation of the ambient field. The white line tentatively indicates the location of the cable (as estimated by Lat-Long coordinates available at the time the cable was laid). The observations suggest that the cable has shifted from its original location, likely through the action of sediment transport.

At the shallow and Barracuda sites, since the water depth was respectively 5m and 10m, a different procedure was used to acquire the emitted EMF data. The SeaSPY magnetometer and the AUV were lowered one at a time to measure and record the B and E fields respectively. The cable was energized with AC (0.98 - 1.59 A at 60 Hz) and DC power (2 – 2.4 Amps) during the monitoring surveys. The measured values of the EMF emitted by the cable in its vicinity at the Barracuda site are provided in Table 1. The measured electric field for the AC current case, exceeding 200µV/m, is significant and within the range 0.5 – 1000µV/m for which responses from elasmobranch species have been observed (Gill and Taylor, 2002). It is believed that the species are attracted by weak electric fields but repelled by strong electric fields. The magnetic field emitted from the cable carrying DC current is significant within 3m distance from the cable.

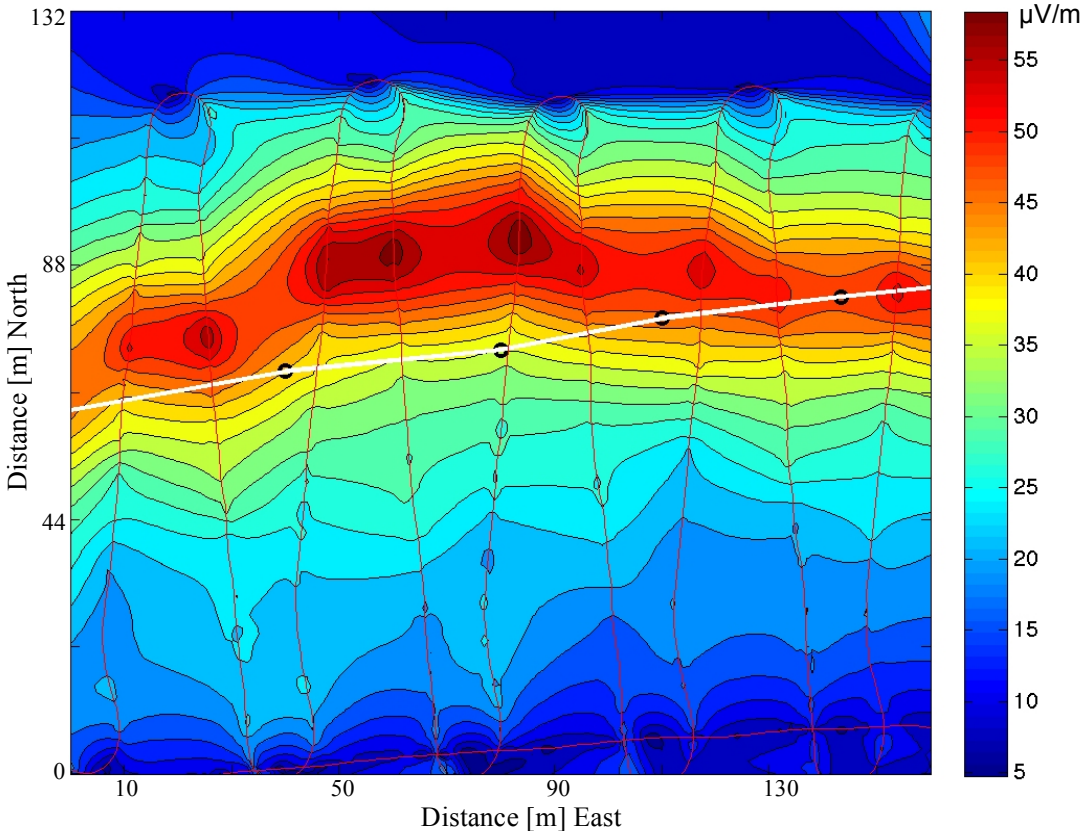

Fig. 19: E-field 4m above a subsea cable energized with 10Hz AC power.

Table 1: Measured EMF emissions from a subsea cable carrying AC and DC cable at the Barracuda site where the water depth is 10m.

Distance from the cable [m]	1.59A AC current in cable @ 60Hz		2.53A DC current in cable	
	Measured magnetic field [nT]	Measured electric field [μV/m]	Measured magnetic field [nT]	Measured Electric Field [μV/m]
0.1	401	-	559	
0.5	195	-	279	
1	78	-	168	
1.6	44	319	110	0
2	33	318	88	0
3	16	305	54	0
4	8.9	290	38	0
5	5.8	271	30	0
6	3.2	254	23	0
7	2.2	234	18	0
8	0.4	225	14	0
9	-	210	-	0
10	-	204	-	0

The electric field was sampled using the custom E-field sensors at a frequency of 2kHz while the magnetic field was sampled at the limited frequency of 1Hz of the available Marine Magnetics magnetometer. The electric field was band pass filtered around the AC frequency of the power source and analyzed. The horizontal component of the E-field, band pass filtered around 60Hz and subsampled at 200Hz, is shown in Fig. 20, together with the signal envelope and the altitude of the AUV above the seabed. The AUV was lowered and raised through the water column over the live cable three times. As expected, the signal level increases when the AUV gets closer to the cable. The surveys were repeated with the power turned off and with DC power in the cable – no induced E-fields were observed in these cases.

The measured data are compared with theory in Fig. 21 where two models (Lucca 2013) are shown, (i) a model that excludes effects of allowing for the presence of the bottom boundary as well as the free surface, and (ii) a model that properly accounts for both boundaries. The models are plotted using a shielding factor of 1.16. As can be seen, there is good agreement between the measured data and model (ii). Electric field in excess of 200μV/m were recorded in the entire water column.

In the case of the shallow site (water depth 5m), the water column appeared saturated and no variation with depth could be discerned (Fig. 22). A mean field of 160µV/m was observed.

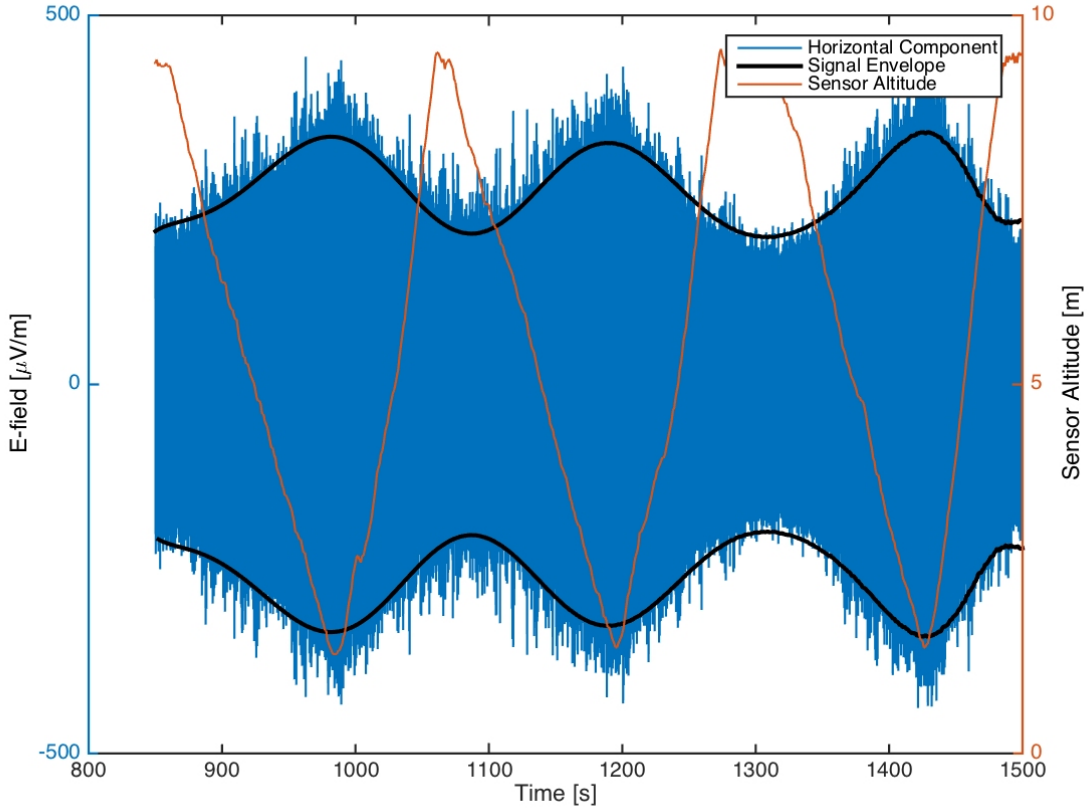

Fig. 20: Variation in horizontal component of the E-field with altitude above the cable as measured with the AUV-based sensors. The cable carried 1.59A AC current at 60Hz.

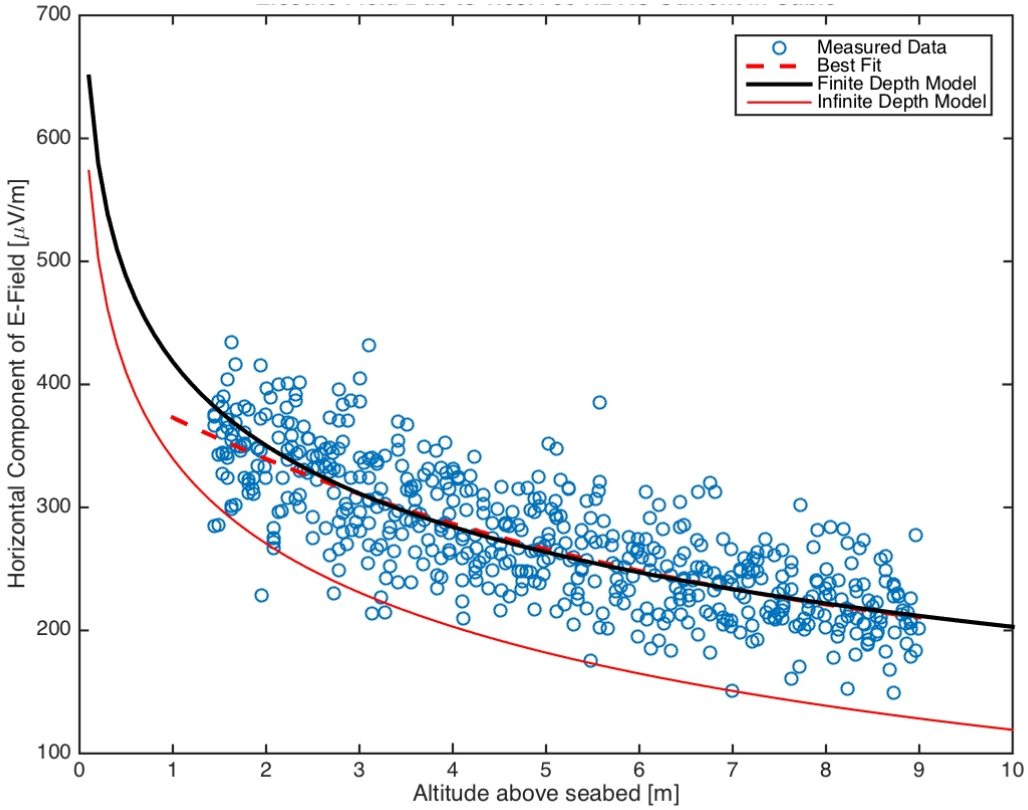

Fig. 21: Comparison of the measured E-field, shown in Fig 20, with theory (Lucca 2013). The measured data correspond to the amplitude of the AC field as characterized by the signal envelope in Fig. 20.

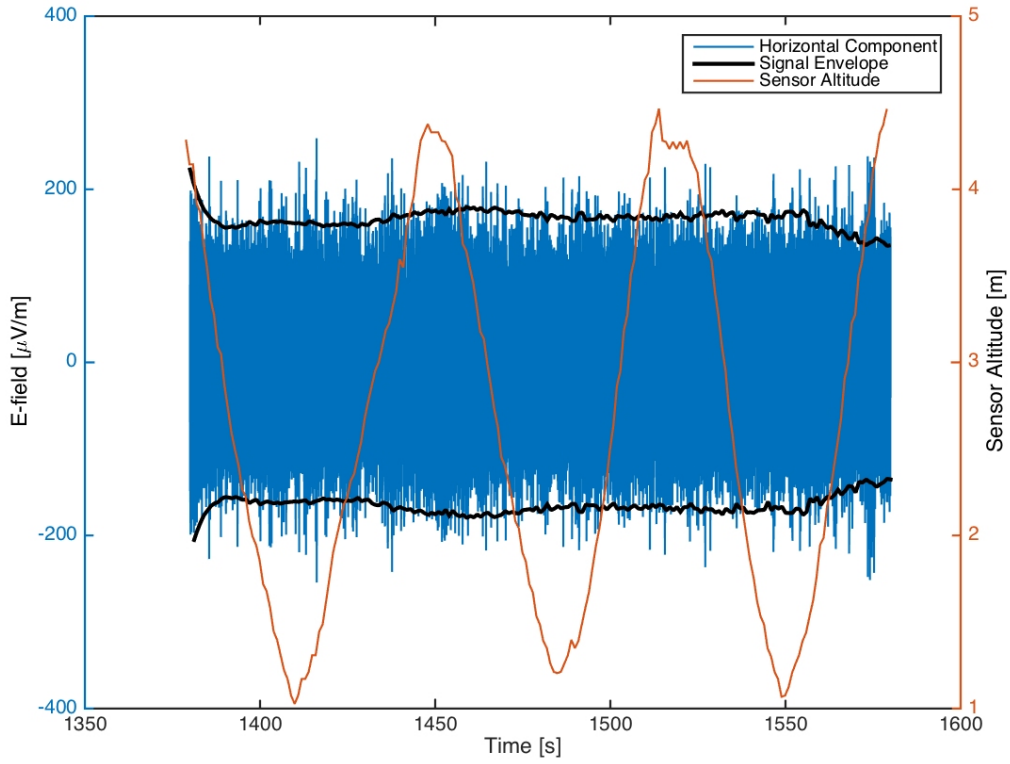

Fig. 22: Observed saturated horizontal component of the E-field in water column above the live cable at the shallow-water site. The power in the cable was 1.59 AC at 60Hz.

The B-field measured at the Barracuda site for a 2.4A DC current is shown in Fig. 23. As before, the magnetometer was lowered and raised through the water column over the live cable three times. The measurements are shown to compare well with theory in Figure 24.

B-field emissions were also recorded in the case of a 1.9A AC current in the cable. The measurements are compared with theory in Fig. 25. The decay rate of the measured B-field is consistent with theory.

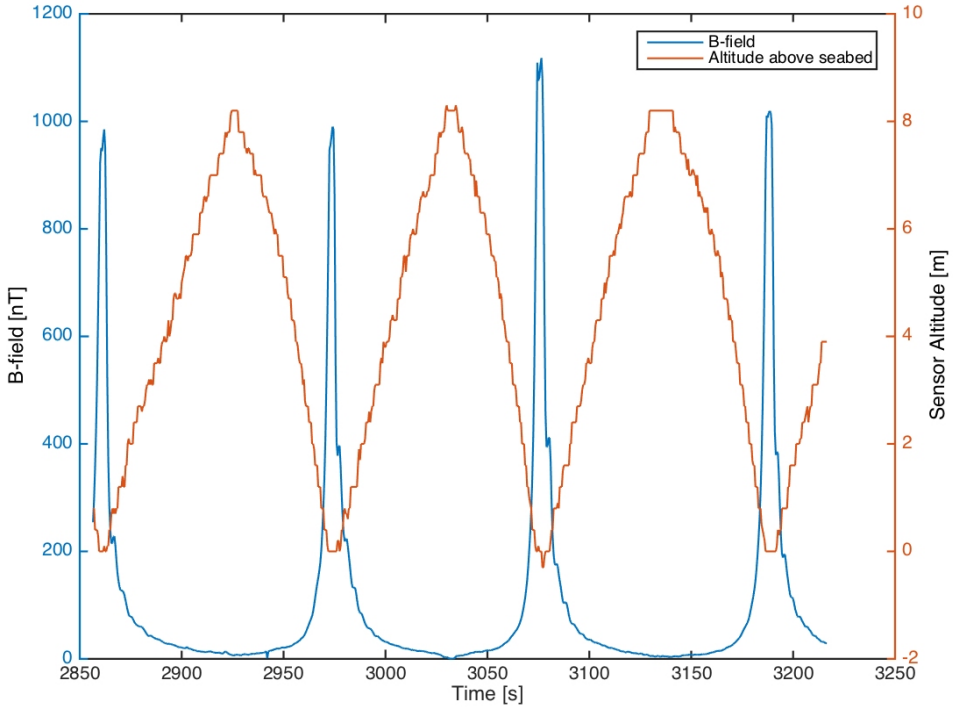

Fig. 23: Variation of the B-field with altitude above seabed for 2.4 A DC power.

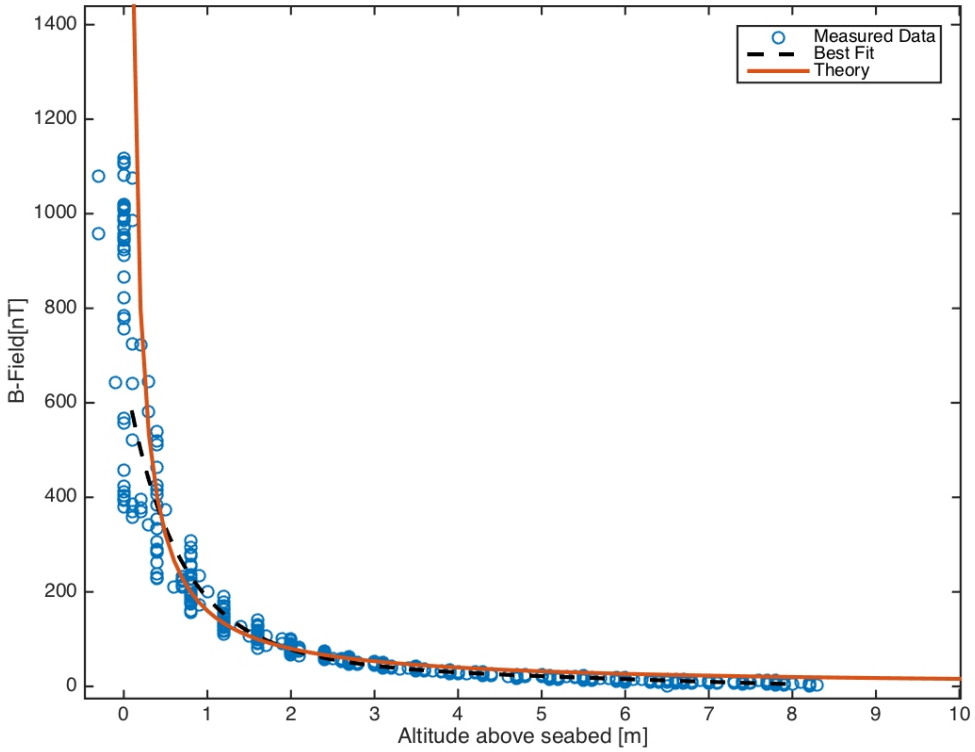

Fig. 24: Comparison of measured data with theory for the case shown in Fig24. A shielding factor of 3 is assumed.

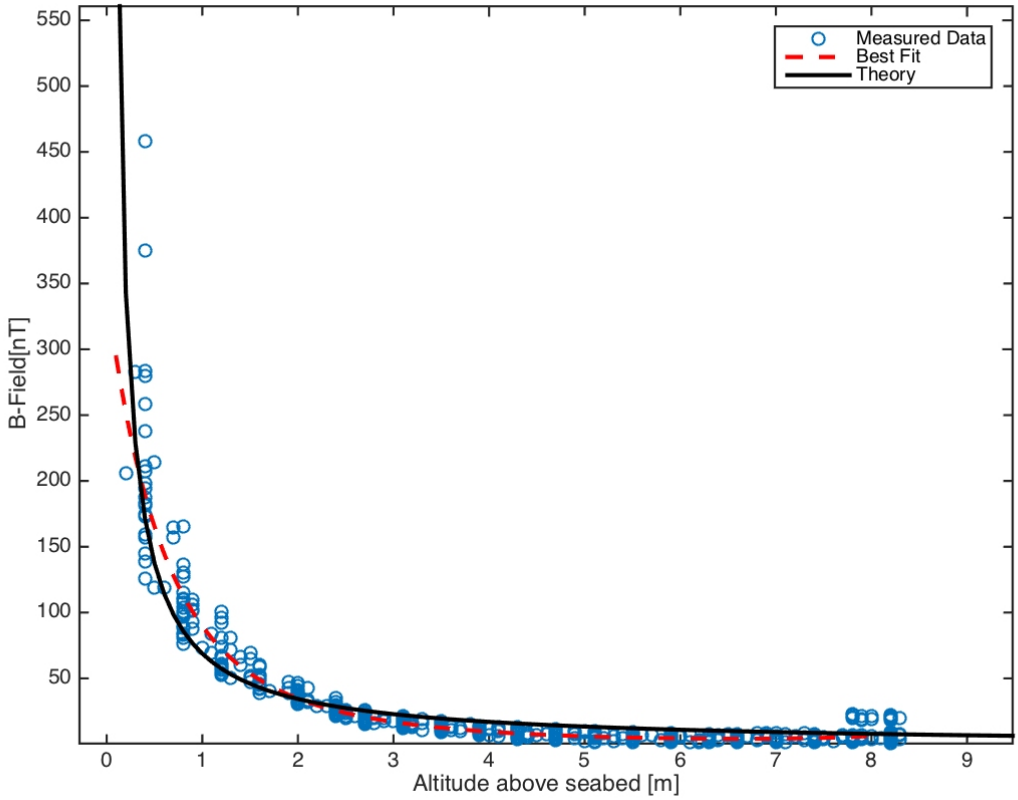

Fig. 25: Comparison of measured B-field data with theory
for a 1.9A AC 60Hz current. A shielding factor of 4 is assumed

VI. Marine Organismal Response to EMF Anomalies

A. Aquatic species surveys by divers on SCUBA Major Activities

During implementation of each quarter's Coordinated Survey Plan, SCUBA divers conducted *in-situ* visual surveys at three sampling locations offshore of the South Florida Ocean Measurement Facility (SFOMF) on an identified cable where AC or DC power could be applied. These sites were designated as Shallow, Middle, and Deep, and were in water depths of approximately 5, 10, and 15 m, respectively. These locations were selected based on their robust reef fish community and are representative of each of the three primary hardbottom coral reef habitats in the local offshore environment: Inner (Shallow), Middle, and Outer (Deep) reef tracts (Banks et al., 2007). Divers on SCUBA primarily assessed the resident coral reef fishes but also transient species including elasmobranchs. SCUBA-based surveys used two standardized methods, stationary point-counts and transect-counts, to record fish species, size, and abundance. In the stationary point-count, all fishes within an imaginary cylinder, 15 m in diameter, that extends from the reef substrate to the water surface, were identified and counted. The diver performed the count by staying in the center of the cylinder and rotating 360° to record species information. For the first 5 minutes of the survey, only species names were recorded. After the 5-min species-count was completed, the total abundance (N) and the mean, minimum, and maximum fork length (FL) for each species were recorded. For the transect-counts, a set of two 30-m sections of the target cable that lay across the appropriate representative habitats at each of the 3 study sites was delineated using a transect tape and subsurface buoys were installed directly on the cable at 7.5 m intervals to mark distance and position along the transects and cylinder center and edge points for the point-counts. In the transect-counts the diver swam along the cable, recording all fishes within 1 m to either side and 1 m above the cable (an imaginary 60 m^3 tunnel). Abundances and fork length (FL) (by size class: <2, ≥2-5, ≥5-10, ≥10-20, ≥20-30, ≥30-50 and ≥50 cm) of fish species were recorded. In both types of counts the diver carried a 1-m ''T''-rod, with the size classes marked off, to aid in fish length and transect width estimation. These two survey methods have been statistically validated and produce data amenable to rigorous statistical analysis, both parametric and non-parametric. The methods are used routinely by NSU researchers and researchers from other organizations to examine both differences in community structure as well as species-specific site differences (Bohnsack and Bannerot, 1986; Baron et al., 2004; Ferro et al., 2005; Brandt et al., 2009; Smith et al., 2011; Gilliam et al., 2013; Kilfoyle et al., 2013).

Two pairs of visual surveys, 2 stationary point-counts and 2 transect-counts, were performed during each segment of a blind randomized sequence of ambient (OFF) and energized AC and DC (ON) cable power states. In addition, survey divers monitored the behavior of the fish community in the immediate vicinity of the cable for "unusual" or unexpected movements or reactions during the exact moment of power transition from ambient (OFF) to energized AC or DC (ON), and vice versa. Prior to beginning surveys at each site, divers positioned tripod-mounted stationary video cameras directly over the cable with the field of view aimed parallel to the axis of the cable to record the movements and behaviors of the fish community. The cameras captured continuous video of the cable and associated fish assemblages at each site, including segments of time during which the *in-situ* visual surveys were being conducted, and

continued until either the camera was recovered at the end of the field effort or the battery power was exhausted for each day of surveys.

In addition, beginning in the 4th quarter, water samples were taken near the cable during the visual surveys for turbidity analysis (Table 2). Readings took place with a turbidity meter in a laboratory setting immediately following each day of the fieldwork.

B. Specific Objectives

Progressive examination of the quarterly sampling results and a final analysis were performed on the dataset to determine if the presence of an SFOMF generated EMF alters: (1) abundance, species richness, and assemblage structure of coral reef fishes, (2) the behavior of fishes including elasmobranchs, and (3) the distribution of marine turtles and mammals. Diver observations were also used in attempt to discern if there were any noticeable organismal responses during the transitional period between ambient OFF to energized AC or DC power states, and video footage was intended to augment the *in-situ* visual survey data and aid in interpretation of the results.

C. Methods: Data Collection, Processing, and Analysis

The results presented here represent combined data from five quarters: Quarter 2 (July 2014), Quarter 3 (September 2014), Quarter 4 (November 2014), Quarter 5 (March 2015), and Quarter 6 (June 2015). No data were collected during the first quarter of the grant as this time was used for project start-up activities, such as: logistical coordination, cable identification, site selection and preparation, and refinement of sampling methods. During the entire study period, a total of 263 surveys were conducted: 132 transect-counts and 131 point-counts; 80 AC counts (40 transects, 40 point counts), 67 DC counts (34 transects, 33 point counts) and 116 OFF counts (58 transects, 58 point counts). Each site had a total of 88 total counts, 44 transect counts and 44 point counts, with the exception of the Deep site which had 44 transect counts and 43 point counts due to inclement weather.

Data recorded during visual surveys were entered into Microsoft Excel and analyzed with Statistica (StatSoft Inc., Tulsa, Oklahoma, USA). Examination of the raw (untransformed) abundance revealed unequal variance between treatments (power: AC, DC, ambient OFF) and, therefore, these data were log(x+1) transformed prior to analysis. A one-way analysis of variance (ANOVA) was performed on the transformed abundance and the untransformed species richness data. If the ANOVA indicated a difference a Student-Newman-Keuls (SNK) test was used to examine differences among treatment means. For examination of assemblage structure, non-metric multi-dimensional scaling (MDS) plots were constructed using Bray-Curtis similarity indices of log(x+1) transformed abundance data (PRIMER v6; Clarke and Warwick, 2001).

As an additional exploratory measure, a selection of hyper-abundant schooling species [Masked/Glass Goby (*Coryphopterus personatus/hyalinus),* Blue Runner *(Caranx crysos),* and Ballyhoo *(Hemiramphus brasiliensi*s)] were removed from a secondary analysis of abundance due to their potential to mask underlying trends or patterns of community structure that might be occurring and to determine whether their removal yields results that lead to more robust conclusions. Removal or treatment of outliers is a commonly employed statistical procedure

that can be particularly useful for the interpretation of summary statistics that may be heavily skewed when extreme values are present. Masked Gobies are a diminutive planktivorous species (Maximum length 4.0 cm TL) (Lieske and Myers, 1994) with limited swimming capabilities that, when present, can occur in shoals numbering in the tens to hundreds. As such they are a species that is easy to over- or under-estimate, potentially making the detection of any calculable or behavioral change in response to EMF alteration more difficult. This species was encountered in almost every survey on the Middle and Deep reef sites, and were the single most abundant species recorded during all power states (23.1% of the combined total). Blue Runner, a fast moving reef-associated pelagic species and the fourth most abundant in this dataset (8.3% of the total), was encountered on multiple Deep site surveys in schools exceeding 800-1000 individuals. Ballyhoo, the 11th most abundant species (1.5% of the total), are often attracted to the upwelling produced by divers' bubbles as they rise to the surface and may congregate in schools of hundreds there.

D. Results

1) Species richness

During the course of this project, a total of 151 species representing 35 families were recorded from all three survey locations (Table 1). When the entire dataset is examined, no significant differences were detected between power states (Nested ANOVA, p = 0.35) (Figure 26).

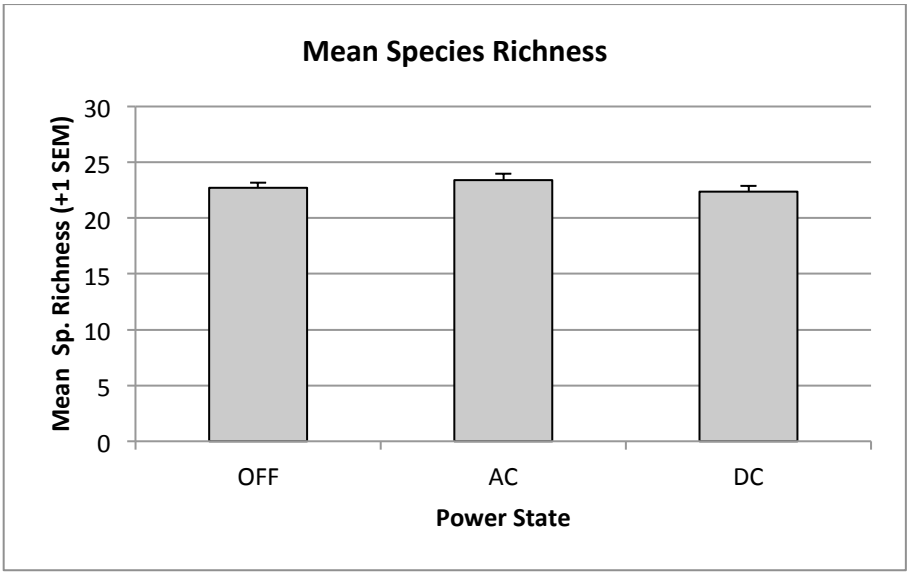

Fig. 26**:** Mean species richness, by power state, using the full data set, during each power state (ambient OFF, energized AC, and energized DC); entire species assemblage with all quarters and sites combined. No significant difference was found (Nested ANOVA, p=0.35). (N = 116 OFF, 80 AC, 67 DC)

The full dataset was broken down further to examine the contribution that each site made to mean species richness. For species richness there were no differences noted among power states within either the Shallow or Middle sites, but curiously there was a difference for the Deep DC (SNK, $p<0.05$, Figure 27). With all power states combined, species richness on the

Deep and Middle sites was significantly greater than on the Shallow site (SNK, $p<0.05$) (Figure 28).

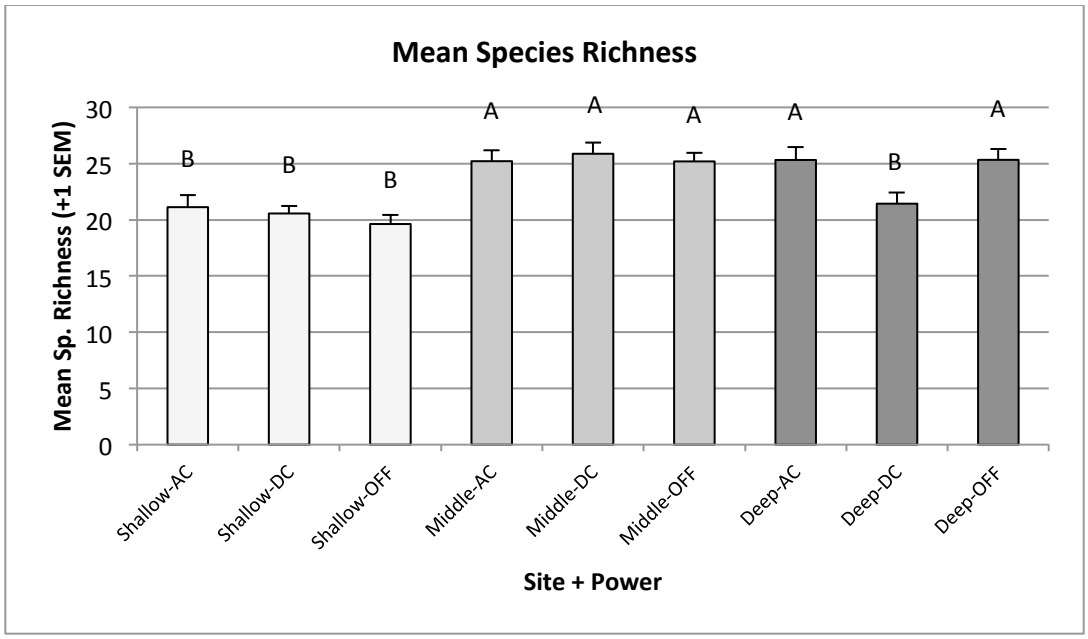

Fig. 27: Mean species richness of fishes, using the full dataset, from each site during each power state (ambient OFF, energized AC, and energized DC); entire species assemblage with all quarters and sites combined. Letters indicate significant differences and shared groupings (SNK, $p<0.05$). (Shallow N = 24 AC, 20 DC, 44 OFF; Middle N = 28 AC, 24 DC, 36 OFF; Deep N = 28 AC, 23 DC, 36 OFF)

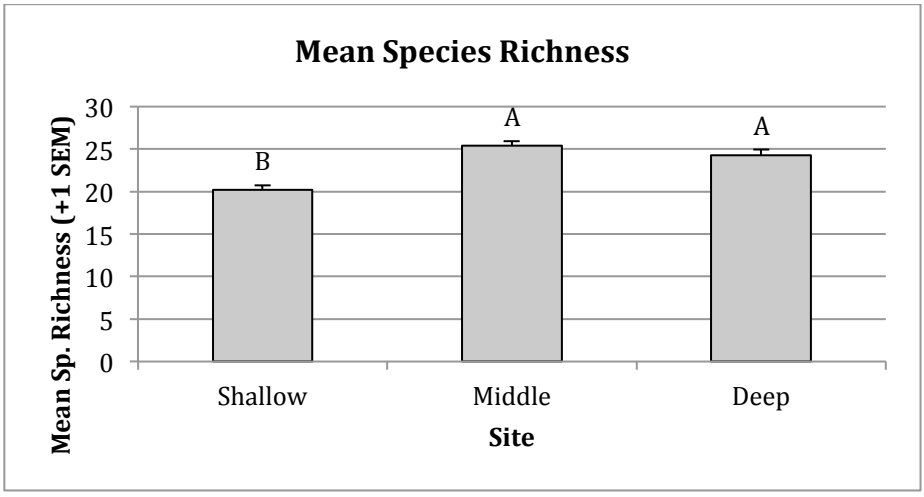

Fig. 28: Mean Species Richness of fishes, by site using the full dataset, with all power states combined; entire species assemblage with all quarters combined. Letters indicate significant differences and shared groupings (SNK, $p<0.05$). (N = 88 Shallow, 88 Middle, 87 Deep)

With the assumption that fishes in closer proximity to the cable receive stronger EMF emissions and might therefore be more inclined to alter their behavior or movements in response, a comparison of point-count to transect-count data was also made and indicated more species were recorded with point-counts (SNK, $p<0.05$) (Figure 29).

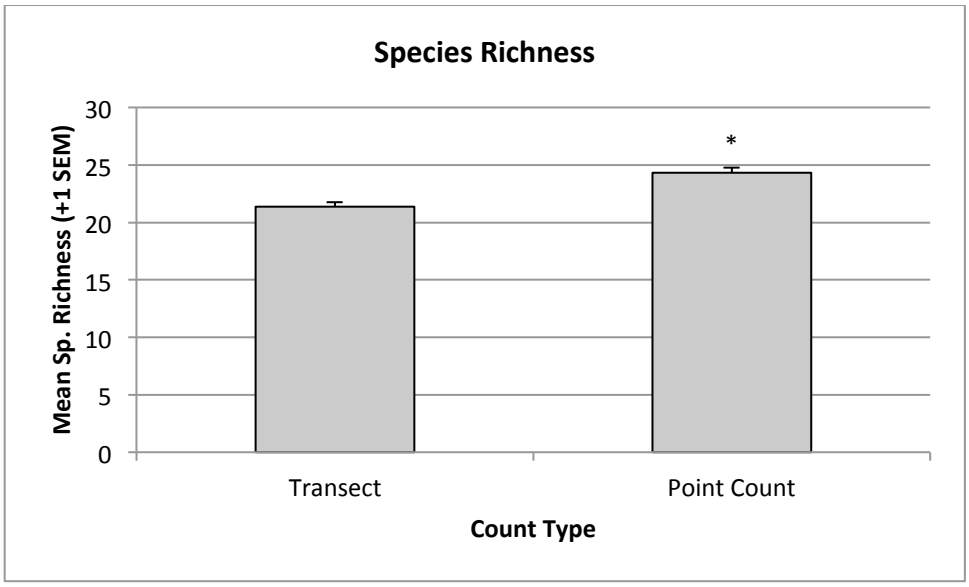

Fig. 29: Comparison of mean species richness of fishes between visual survey types. The asterisk signifies a significant difference (SNK, $p<0.05$). (N = 132 Transect, 131 Point-count)

Few species were recorded only in one power state. Of the 29 species that were found only in a single power state, 13 were only counted once as individual fish, and the rest were isolated occurrences of 2-5 individuals or in a single count (i.e., a school of 30 Lane Snapper) (Table 1). Slightly more of these species were found during ambient (OFF) conditions (13), than in the other power states (AC 11 total, DC 9 total). Only two elasmobranch species were encountered during the visual surveys, the Yellow Stingray (*Urobatis jamaicensis)* and Southern Stingray (*Dasyatis americanus*). The Yellow Stingray was counted exclusively during ambient (OFF) conditions, although only 5 individuals were recorded. The Southern Stingray was counted once during energized AC (ON) and once during ambient (OFF) conditions. No turtles or marine mammals were encountered.

2) Abundance

There were 24,473 fishes counted during transect-count surveys. When the abundance by power state is standardized by the relative number of samples taken within each power state, 44% of the fishes were counted during ambient (OFF) surveys compared to 29% for AC and 27% for DC. For point-counts, 36,115 fishes were counted, 39% of which were during ambient (OFF) surveys compared to 33% for AC and 28% for DC (Table 1). Although more fish were recorded during the ambient (OFF) sequences for both count types, with all quarters and sites combined there were no statistical differences detected (ANOVA, $p = 0.21$) (Figure 30). Likewise, on a quarterly basis the abundance of fishes did not differ significantly among power states (ANOVA, $p>0.05$) (Table 4). Note the figures for abundance were generated using untransformed

abundance data to provide a visual comparison of means, whereas the ANOVAs used to test for differences between the means were performed with transformed data. When the modified dataset is examined (with select gobies, jacks, and ballyhoo removed), visually, the abundance relationships between the power states are balanced more equally and remain statistically non-significant (ANOVA, p=0.81) (Figure 31). However, it is noteworthy that the greatest total abundance in both transect-counts and point-counts was recorded during ambient (OFF) conditions (Figures 30 and 32). Likewise, fish density was higher during ambient (OFF) conditions (Table 3).

The largest percentage of species recorded during this study, from both count types combined, had their highest abundance during ambient (OFF) conditions (AC 33%, DC 25%, OFF 42%; ANOVA, p<0.0001). When the percent distribution by species was examined by power state with each count type combined, the majority of species recorded during this study had significantly higher abundance during ambient (OFF) conditions (AC 33%, DC 25%, OFF 42%; ANOVA, p<0.0001) (Table 3). There were 24 species with higher abundances recorded from both count types during ambient (OFF) conditions, and the total number of fishes counted during OFF conditions comprises 40.9% of the total recorded during the entire project for all power states. Comparatively, there were only 10 species that had higher numbers for both count types in AC and 9 species for DC, comprising 31.6% and 27.6% of the total abundance, respectively. Comparatively, there were only 10 species that had higher numbers for both count types in AC and 9 species for DC, comprising 31.6% and 27.6% of the total abundance, respectively.

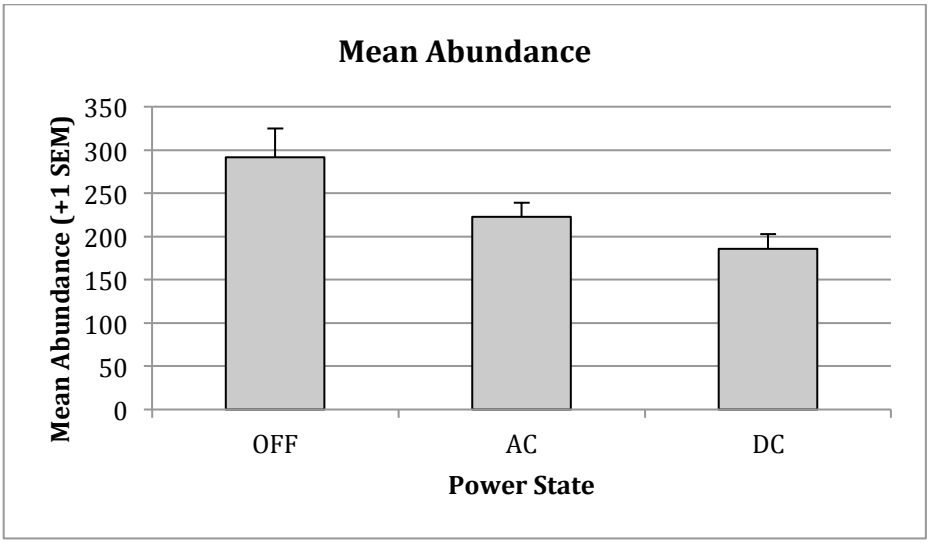

Fig. 30: Mean abundance of fishes, using the full data set, during each power state (ambient OFF, energized AC, and energized DC); entire species assemblage with all quarters and sites combined. No significant difference was found (ANOVA, p=0.21). (N = 116 OFF, 80 AC, 67 DC)

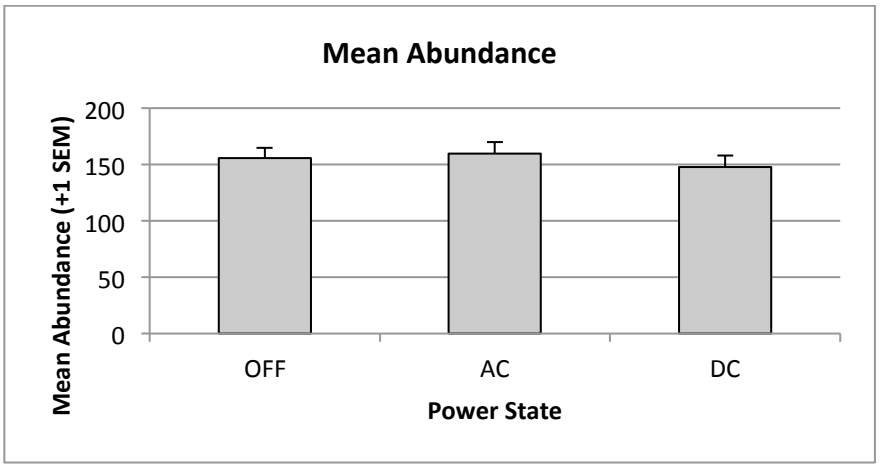

Fig. 31: Mean abundance of fishes, using the dataset with Masked/Glass Goby, Blue Runner and Ballyhoo removed, during each power state (ambient OFF, energized AC, and energized DC); all quarters and sites combined. No significant difference was found (ANOVA, p=0.81). (N = 116 OFF, 80 AC, 67 DC)

When the dataset is broken down further to examine the contribution each site made to mean abundance, there were minor differences between power states at the Shallow site, but the Middle and Deep sites had greater values during ambient OFF conditions (SNK, $p<0.05$) (Figure 32). Also, using the modified dataset (with Masked/Glass Goby, Blue Runner, and Ballyhoo removed), no significant differences were noted for abundance (Figure 33) at the Shallow and Middle sites, but Deep OFF once again stands out with slightly greater values (SNK, $p<0.05$). As was also the case with species richness, comparison of count types indicated more fishes were recorded with point-counts than with transect-counts (SNK, $p<0.05$) (Figure 29, 36).

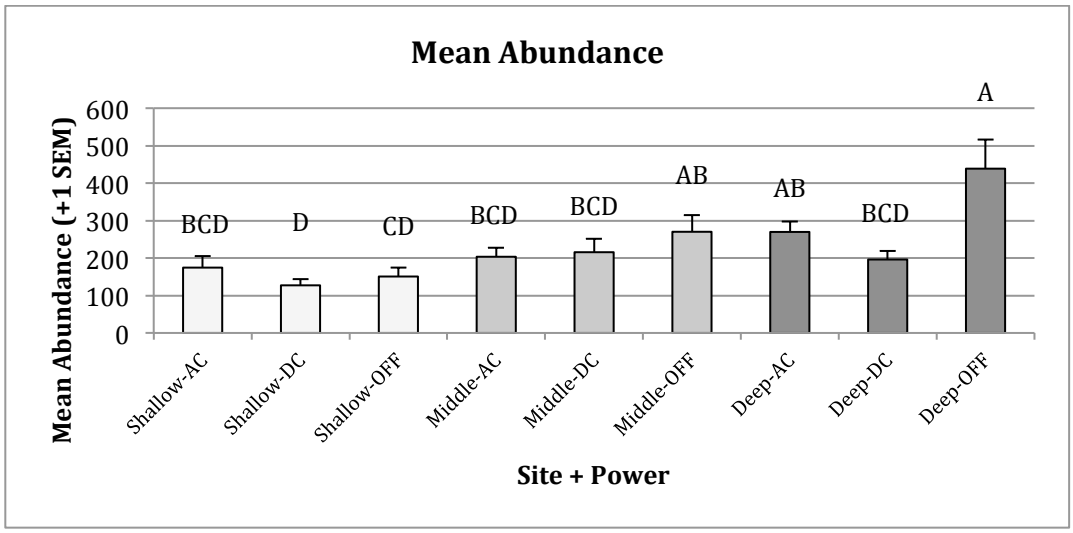

Fig. 32: Mean abundance of fishes using the full data set, from each site during each power state (ambient OFF, energized AC, and energized DC); entire species assemblage with all quarters and sites combined. Letters indicate significant differences and shared groupings (SNK,

p<0.05). (Shallow N = 24 AC, 20 DC, 44 OFF; Middle N = 28 AC, 24 DC, 36 OFF; Deep N = 28 AC, 23 DC, 36 OFF)

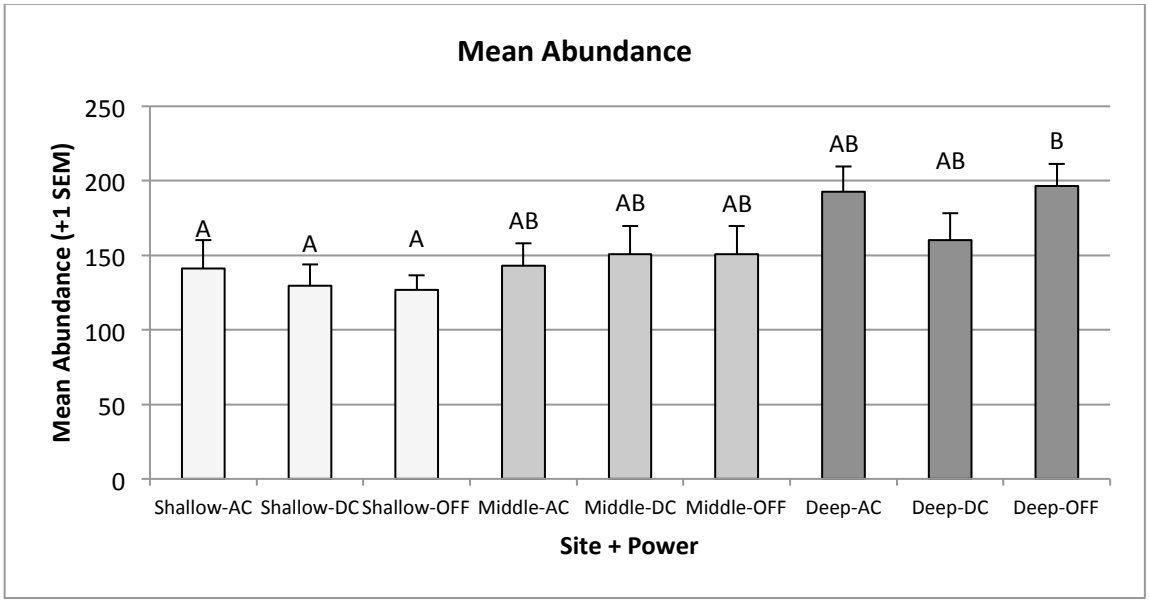

Fig. 33: Mean abundance of fishes, using the dataset with Masked/Glass Goby, Blue Runner and Ballyhoo removed, from each site during each power state (ambient OFF, energized AC, and energized DC); entire species assemblage with all quarters and sites combined. Letters indicate significant differences and shared groupings (SNK, p<0.05). (Shallow N = 24 AC, 20 DC, 44 OFF; Middle N = 28 AC, 24 DC, 36 OFF; Deep N = 28 AC, 23 DC, 36 OFF)

If, for abundance, all power states are combined, both versions of the dataset (complete and modified) had, like richness, differences among sites and were significantly greater at the Deep site (SNK, p<0.05) (Figures 34 and 35).

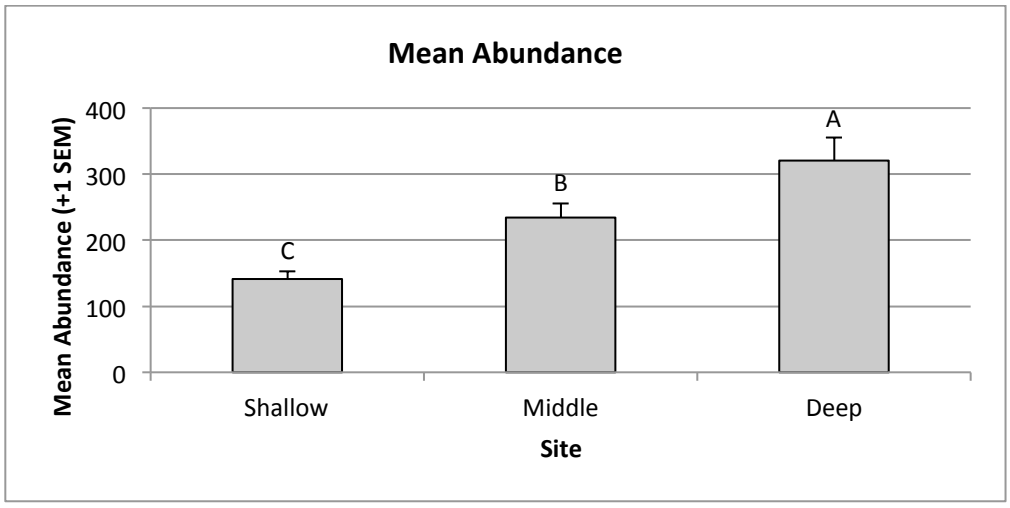

Fig. 34: Mean Abundance of fishes, using the full dataset, from each site with all power states combined; entire species assemblage with all quarters combined. Letters indicate significant differences and shared groupings (SNK, p<0.05). (N = 88 Shallow, 88 Middle, 87 Deep)

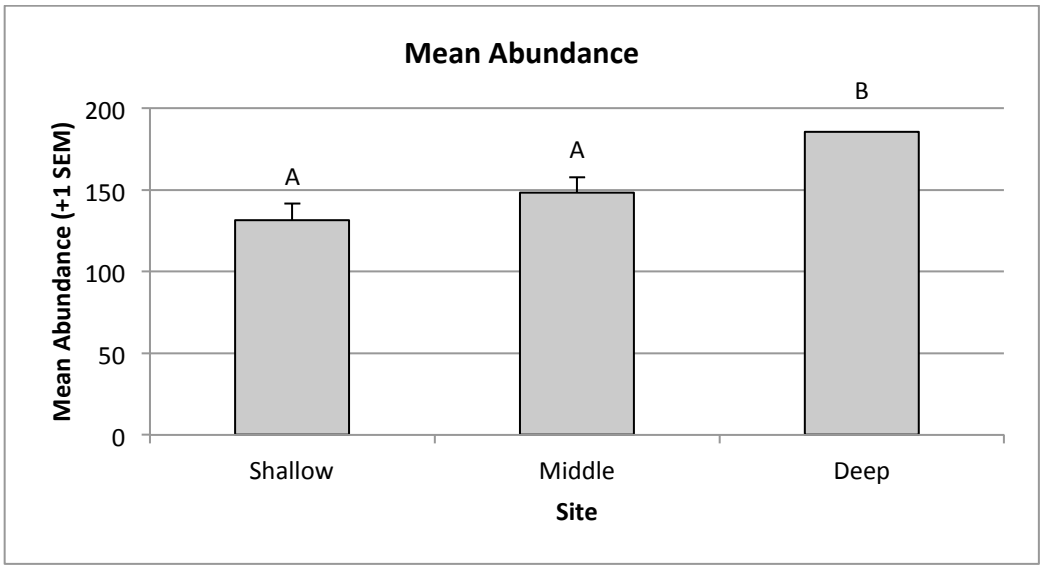

Fig. 35: Mean Abundance of fishes, using the dataset with Masked/Glass Goby, Blue Runner and Ballyhoo removed, from each site with all power states combined; entire species assemblage with all quarters combined. Letters indicate significant differences and shared groupings (SNK, $p<0.05$). (N = 88 Shallow, 88 Middle, 87 Deep)

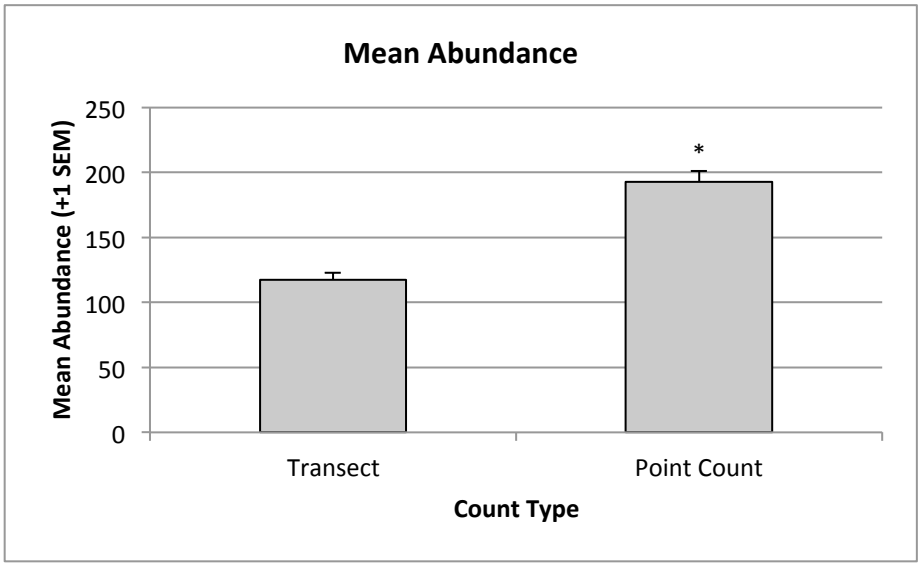

Fig. 36: Comparison of mean abundance of fishes between visual survey types (SNK, $p<0.01$). (N = 132 Transect, 131 Point-count)

3) Community analysis

Assemblage structure was examined with both versions of the dataset (with and without selected species), but results revealed that the patterns of distribution among samples were nearly identical and only the full dataset is presented here. The site differences that were previously noted for richness and abundance (Figures 28, 34, and 35) are also echoed here, with clear separation occurring for each site (Figures 37-41). When all sites and count types are combined, no distinct clustering of assemblage structure can be attributed to any of the

individual power states (Figures 38 and 39). However, it does appear that in general the distribution for ambient (OFF) counts was slightly more spread out than either energized AC or energized DC, especially at the Shallow and Deep reef sites.

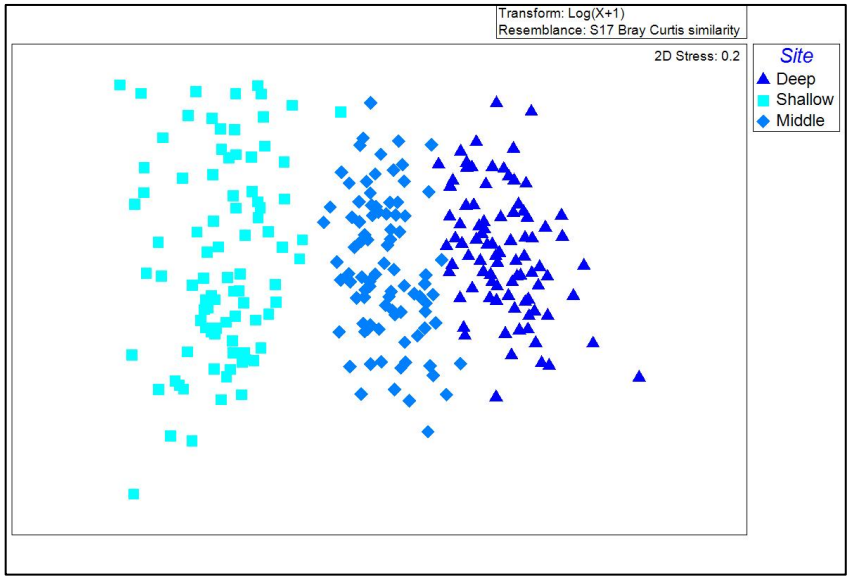

Fig. 37: MDS plot of fish assemblages by reef-tract site, all power states combined. The three sites are clearly separated. (N = 88 Shallow, 88 Middle, 87 Deep)

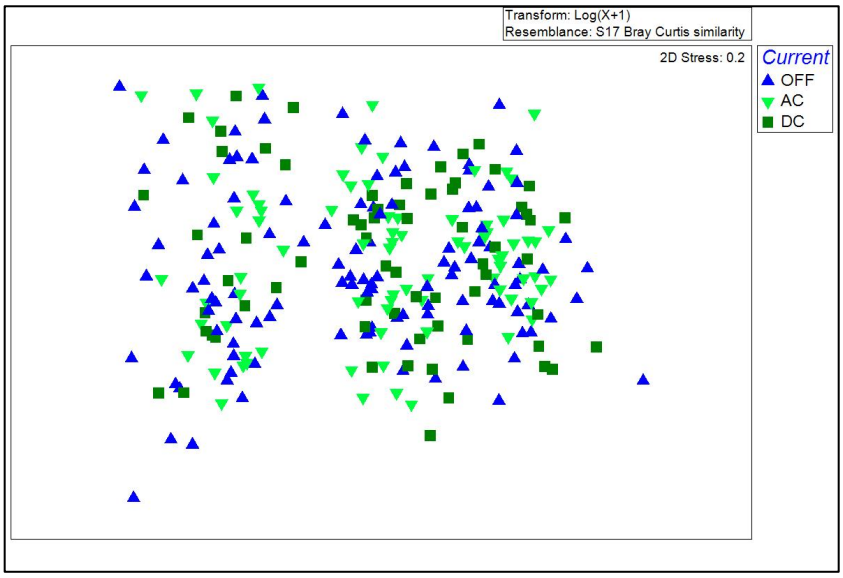

Fig. 38: MDS plot of fish abundance by power state (OFF, AC, and DC) for all sites. (N = 116 OFF, 80 AC, 67 DC)

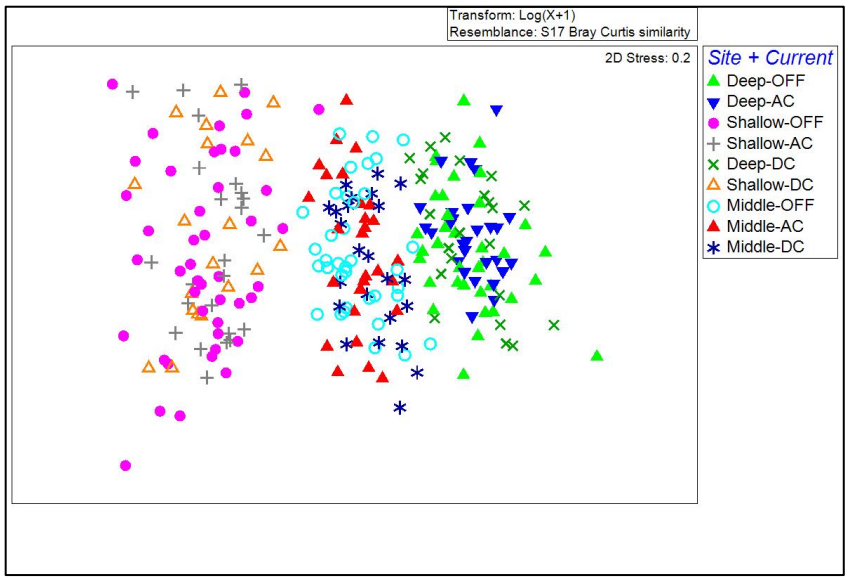

Fig. 39: MDS plot of fish assemblages comparing site and power state (OFF, AC, and DC) for each site. (Shallow N = 24 AC, 20 DC, 44 OFF; Middle N = 28 AC, 24 DC, 36 OFF; Deep N = 28 AC, 23 DC, 36 OFF)

Distribution of the points for each count type (Figure 40) suggest that point-counts and transect-counts are characterizing separate but slightly overlapping components of the same assemblage, which is to be expected given the nature of each of these two methodologies. When transect-count and point-count count data are analyzed separately (Figure 41), once again a similar pattern of indistinct clustering is noted, which leads to the conclusion that there is limited evidence for differences in community structure between power states as they were examined here on a community-level scale.

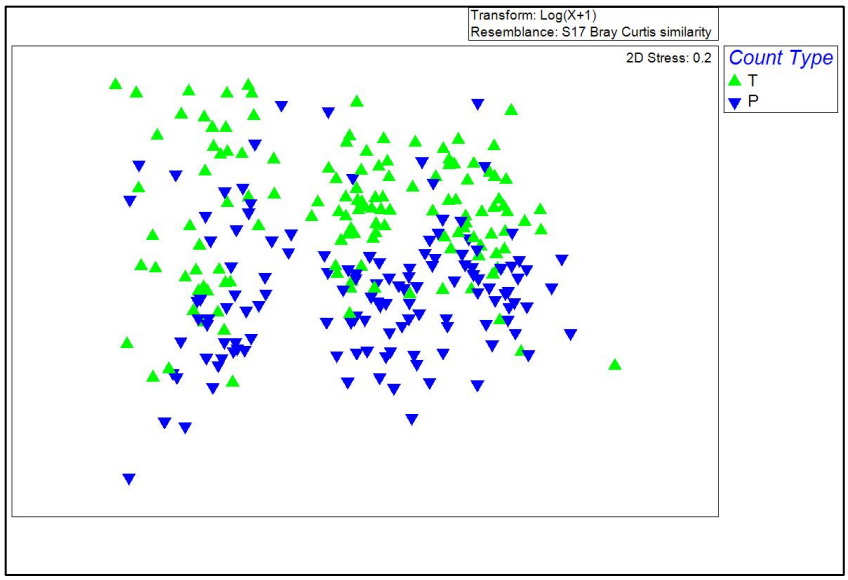

Fig. 40: MDS plot of fish assemblages comparing transect-counts (T) to point-counts (P). (N = 132 Transect, 131 Point-count)

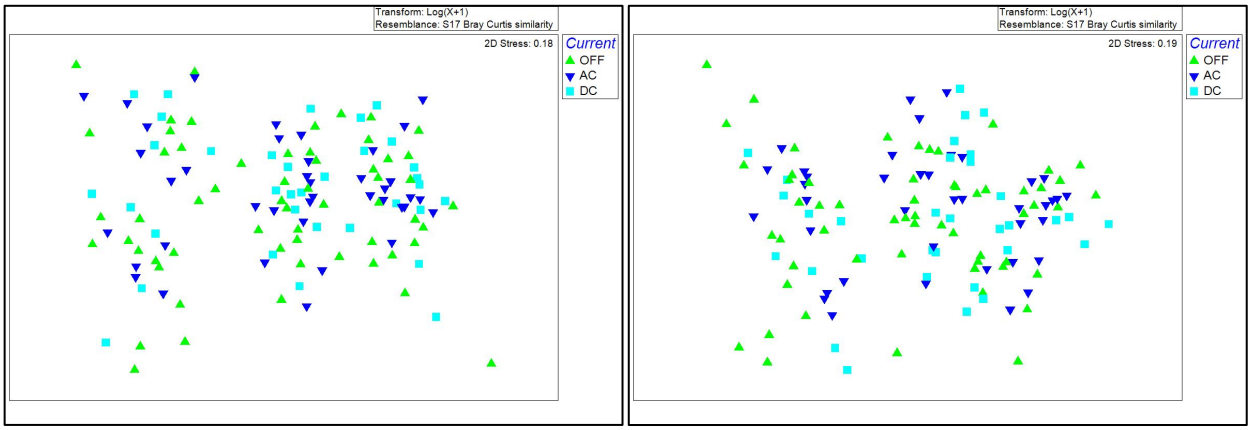

Fig. 41: MDS plot of fish assemblages by power state, transect-count only (left) and point-count only (right). (Transect N = 58 OFF, 40 AC, 34 DC; Point-count N = 58 OFF, 40 AC, 33 DC)

4) Behavior

In order to make *in-situ* observations of fish movement and behavior at the exact moment of power transition, divers were positioned along the cable prior to each power transition from ambient OFF to energized AC and energized DC and vice versa, although the survey divers were unaware of what the power state was for any given power transition due to the blind survey design. No detectable behavioral responses of fishes or other organisms to power transitions were observed at any of the 3 survey locations.

E. Stationary video

An analysis of the stationary video footage was attempted, however positive identification and quantification of the fishes within the field of view proved to be problematic and generation of data that could be used to evaluate the fish community on a similar scale as that generated from the *in-situ* visual surveys was not achieved. Sample images from the video footage are shown in Figure 42. Multiple methods, such as taking a snapshot of the video at pre-determined time intervals and magnification of select areas during the video analysis, were utilized with limited success. Underwater visibility (i.e., water clarity and turbidity), distance from the camera to the targets (fishes), and camera resolution were contributing factors that resulted in only a rudimentary identification and quantification of the fishes that were present during each power sequence. Accurate assessment by the video observer was possible for those fishes that were observed within a range of minimum proximity to the camera, fish size, and swimming speed. However, it was decided that the accuracy of assessment did not extend far enough to include the majority of the fishes that were actually present within the field of view during the surveys. Detectable behavioral responses of other organisms (marine mammals, turtles) to power transitions were also not observed in the stationary video footage.

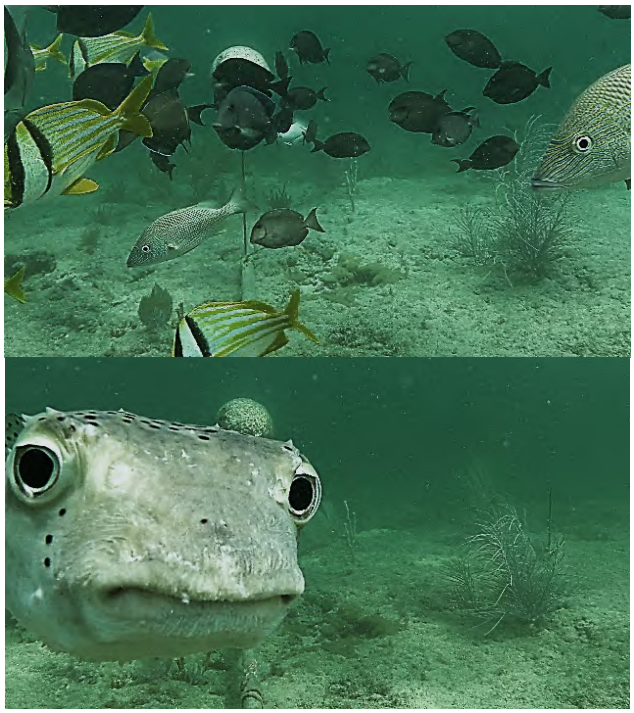

Fig. 42: Views from the stationary underwater video.

F. *Turbidity Measurements*

The turbidity measured in the water column during the surveys are provided in Table 2 below:

Table 2: Turbidity readings in Nephelometric Turbidity Units (NTUs) taken near the cable during SCUBA surveys.

Date	Quarter	Site	Mean Turbidity (±SEM)
3/17/2015	4	Middle	0.34 ±0.11
3/31/2015	4	Shallow	0.18 ±0.04
4/2/2015	4	Deep	1.92 ±0.04
6/9/2015	5	Deep	1.34 ±0.10
7/20/2015	5	Shallow	6.73 ±0.11

G. *AUV-based video observations*

Figures 43a and 43b illustrate observations from the AUV and the magnetometer based video cameras respectively. The videos, the mounting configuration, video analysis and associated discussion are included in the database.

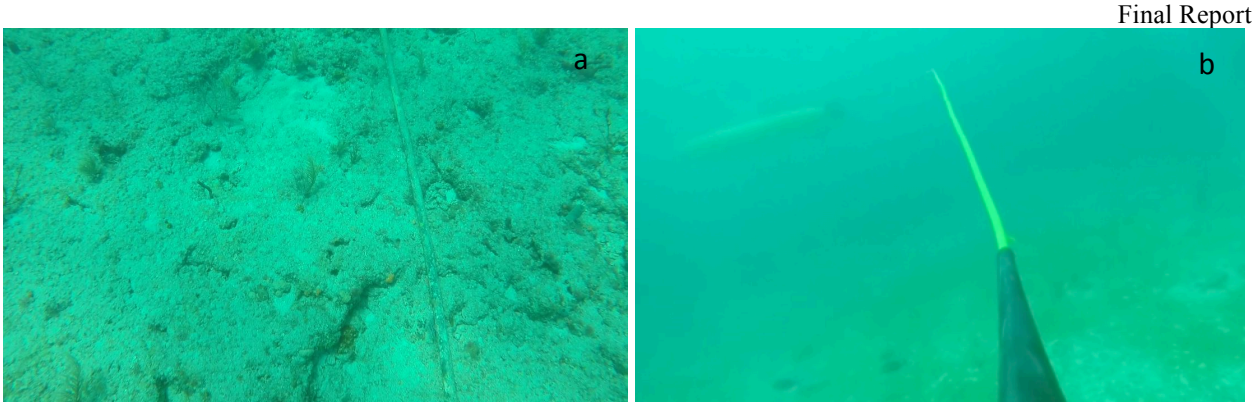

Fig. 43 (a) View from AUV video camera during a mission over the cable. (b) View from the magnetometer based video camera.

No significant conclusions could be made from the AUV-based cameras in view of (a) limited data (b) possible intrusion effect, (c) coverage issues. Sightings of animals were recorded, although species could not always be identified. Figures 44 illustrate abundance counts based on analysis of the videos. Figure 45 maps the animal sighting relative to the cable for various power states. Additional data are provided and videos are provided as part of the database that is developed.

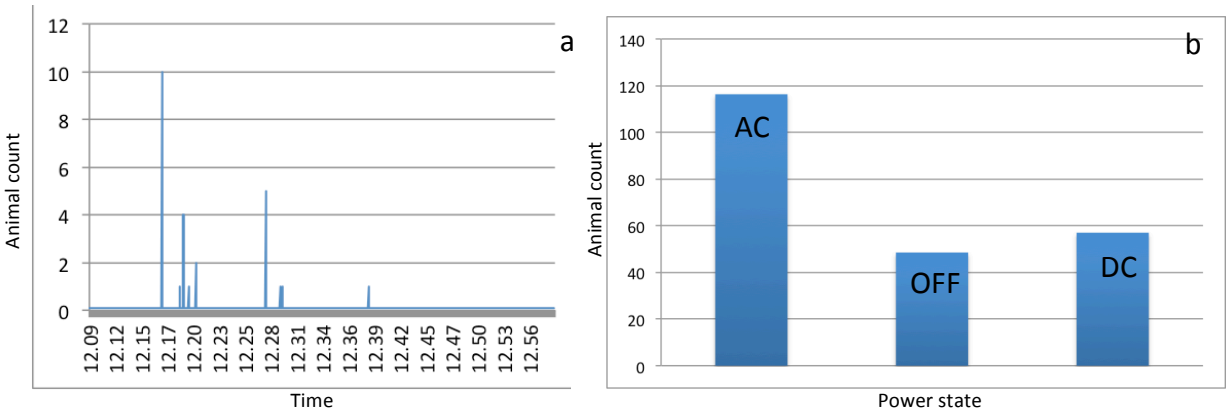

Fig. 44: (a) Representative animal count at the deep site from AUV-based video during a lawn-mower pattern survey mission over the cable carrying 10Hz AC power, (b) Mean animal count over several missions for different power states at the deep site.

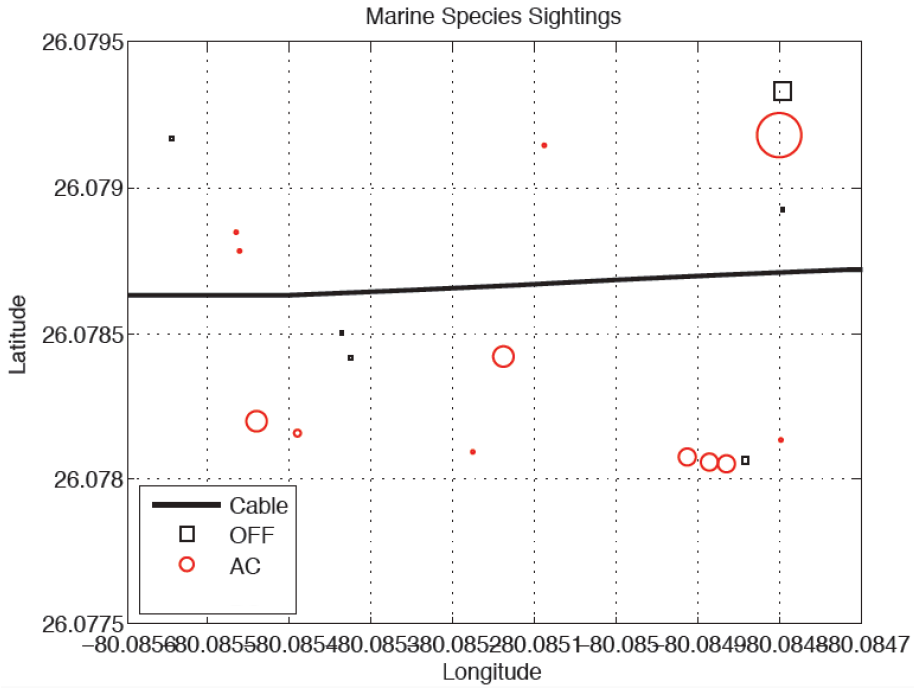

Fig. 45: Abundance observations such as in Fig. 44a qualitatively mapped onto the deep-site region in the vicinity of the cable for different power states. The size of the symbols depicts relative level of abundance.

VII. Discussion

EM field sensors, including a SeaSPY magnetometer and a custom E-field sensor, have been implemented on a Bluefin 21 AUV. The SeaSPY is towed 10m behind the vehicle while the 3-axes Ag/AgCl E-field sensor is located on the AUV. The measured data are processed, digitized and stored on board the AUV together with data from other sensors. The buoyancy and trim of the vehicle as well as the electric ground arrangement on the standard SeaSPY had to be modified as part of the implementation. The sensor tows well and analysis of the results suggest that good quality measurements can be made using the arrangement discussed here. Recent modifications allow simultaneous measurement of the E and B-fields during a single mission. Procedures have been developed for measuring background EMF and emissions in the water column from submarine sources using the mobile AUV sensor platform. EMF sensing surveys were conducted with power in the cable turned on (AC and DC) and off. The EMF observations are in good agreement with theoretical models that take proper account of the presence of the free surface and the bottom boundary (Lucca 2013), particularly in shallow water environments. The measurements will help validate various predictive models of the EMF emissions from submarine cables. Additional details are provided as part of the general database, which will serve to support validation of predictive models of the EM emissions from submerged cables. In particular, this study and validated models help the MHK industry in removing deployment barriers through retiring or mitigating environmental risks.

The site dependent differences in fish richness, abundance, and assemblage structure with the power states combined noted here (Figures 28, 34, 37) are likely the result of species-specific

habitat preferences and habitat differences between sites and not due to EMF influences. These site-dependent results are supported by multiple previous data-rich studies in the local area, including those distant from any likely SFOMF influence (Ferro et al, 2005; Gilliam et al., 2013; Kilfoyle et al., 2015).

Likewise, the differences noted between point-counts and transect-counts in richness and abundance, with sites and power states combined, are supported by other studies (Baron et al., 2004). These differences are expected and mainly due to biases of the survey types, not EMFs, and are the underlying reason for using two different methodologies. Interestingly, in this study there was greater species richness and abundance in the point-count, as typically the transect-count records a higher number of species than the point-count. The transect-count is carried out close to the cable, targeting a greater constituency of small, cryptic species and juveniles and may effectively exclude or miss many of the highly mobile species that routinely inhabit the water column. Greater total abundance per count is typical of the of point-count surveys as the diver is assessing a greater surface area and volume than transect-counts (176.7 m^2 and 60 m^2, respectively).

In terms of richness, it does not appear that power state had a strong overall impact. There was no statistical difference in mean richness among the power states and, with some exceptions, individuals within a species were not restricted to a single power state (Table 1). These results appear to be in accord with the absence of noting any immediate change in behavior with the onset of an EMF stimulus. There was no apparent EMF impact on a population severe enough to provoke an immediate movement towards or away from a particular EMF. The exceptions were restricted to rare occurrences of primarily single encounters and often of single individuals. Nonetheless, it is noteworthy that few elasmobranchs, or other fishes known to be sensitive to E or M fields, were counted during the study. Only 2 species of stingrays were recorded. One of those, the yellow stingray, was only counted in the OFF power state. The yellow stingray is known to be electrosensitive in the range of the SFOMF EMFs and may have been avoiding charged cables. However, with only 5 individuals recorded in total this must remain speculation until further research provides additional evidence.

In terms of abundance, our conclusions are not as straightforward as the analyses do not provide for a single clear interpretation of the data. Although when graphed the means for the full study (5 quarters) appear different, the ANOVA analyses of the transformed data do not indicate statistical differences among the power states (Figures 30, 31). However, fish abundance data acquired from visual surveys is typically characterized by high variability, and this dataset is by no means an exception. The low number of counts examined and the high variability within counts provides a high probability of a Type II statistical error (experimental design had a power of 0.7), finding no difference among power states when there is one. Thus, we caution some discretion in reaching a concrete conclusion based solely on the ANOVA results. More fishes were recorded in the OFF power state (interestingly with an ANOVA of the untransformed data this difference was significant ($p=0.035$), and if abundance is examined from a species perspective, more species had their highest number of individuals recorded during the ambient (OFF) state and abundance calculated as percent species population (the

distribution of each species within the three power states) was higher during the power OFF condition (Table 1).

These disparate analyses are not easy to reconcile. With the caveat that this study may have inadequately counted, or missed completely, some cryptic and transitory species and that we cannot speak to long-term impact on the community, it appears that species richness and the assemblage structure of resident fishes were likely not immediately altered by the short-term changes in the EMFs utilized in this study (Figures 26, 27, 38, 39). Also, no behavioral changes were noted in immediate responses to alterations in the EMF. With no difference in richness, structure, and behavior of fishes detected, and given that the literature does not provide much evidence for fishes being EMF-sensitive, excluding elasmobranchs or diadromous species, it would be easiest to conclude that the EMFs assessed in this study do not impact coral reef fishes and ascribe the contradictory interpretations to problems in analysis or research design. However, the number of times when abundances were highest during power-off in this blinded study begs the question (Table 3). Thus, although we found no evidence for overt discrete changes in behavior, our data do suggest that the artificial EMF may have led to an overall subtle avoidance of the area affected by the EMF stimuli, leading to possible differences in the distribution of fishes.

In addition to potential emigration out of the area, fishes that remain in the area might also be exhibiting differences in behavior, which would influence their being counted, such as remaining closer to the substrate or taking refuge within the reef when EMF emissions are present. If some species are induced to move as a result of the EMF signal, it could potentially be due to an active avoidance of, or escape from, the EMF due to direct aversive consequences on the organism, or it may be due to a process that involves a gradual moving to/from the area in response to subtle EMF effects on various, less obvious, factors. This accords with other studies conducted with a variety of vertebrates, including fishes, exposed to various levels of EMF emissions in laboratory experiments. In a host of studies, often inconclusive or contradictory, EMFs have been shown to influence variables such as: orientation (Putman et al., 2014), enzymes (Li et al., 2014), hormones (Lewczuk et al., 2014), metabolism (Wang et al., 2016), nerve function (Chagnaud et al., 2008; Varro et al., 2009; Tabor et al., 2014), anxiety (Lee and Yang, 2014), development and mortality (Krylov et al., 2016), activity level (Varanelli and McCleave, 1974; Ward et al., 2014; Lee et al., 2014) or hyperalgesia (Jeong et al., 2005), paresthesia (Sugishita and Takayama, 1993) etc. (for additional references see: Öhman et al., 2007; Lee and Yang, 2014; Lewczuk et al., 2014; Pall 2015). Our study does not provide adequate information to form a viable hypothesis regarding the biological mechanism(s) determining any EMF impact. However, clearly impacting any of the variables above could alter distribution.

In conclusion, much of the literature dealing with EMF effects on vertebrates can be summed up as contradictory or inconclusive. This study is in some measures likewise. There are some caveats to consider. We did not see adequate numbers of some species, especially elasmobranchs, known to reside in or transit the area. Thus, some local species might be impacted but our results would not clearly show it. Also, we cannot discount the possibility that the time intervals between power states utilized here (approximately 30 minutes) to assess

changes in reef fish populations was too short to capture slow changes that may be occurring as a result of altering the power state and the low sample sizes and high count variability may be obscuring some statistical analyses. These caveats notwithstanding, we did not find that the EMF provided at the SFOMF had statistically significant impact on the fish assemblage we examined. Nonetheless, although no behavioral effects were noted, the distribution data suggest need for further research to assess the characteristics of subtle impacts. For example, subtle changes in place preference may result from EMF-induced changes in orientation, anxiety, temperature, etc. The potential long-term effect of such impact, if any, on the distributions of fish populations and community structure is not known and further research is needed. Additional studies involving larger sample sizes, longer time intervals with the power remaining constant for each particular current type (OFF vs AC vs DC), different power, and sites are required. Because the potential sensitivity of most non-elasmobranch fishes to EMFs appears low, combining such field studies in conjunction with laboratory behavioral studies would likely produce more conclusive results.

Table 3**:** The total abundance (raw/standardized by sample size/percent within count type) of each observed species across all power states and count types, totals from each energized power state (AC and DC) and ambient (OFF). Sample size differed among count types and power states: Transect-counts: (132) AC N=40, DC=34, OFF=58; Point-counts: (131) AC N=40, DC=33, OFF=58. Shaded cells indicate highest counts by power state within a species for each count type. Species names displayed in bold were seen exclusively in one power state.

Species List			Transects			Point Counts		
Common Name	**Scientific Name**	**Total**	**AC**	**DC**	**OFF**	**AC**	**DC**	**OFF**
STINGRAYS	**DASYATIDAE**							
Southern Stingray	*Dasyatis americana*	2 / 1.4	1 / 0.8 / 59.1	0	1 / 0.5 / 40.8	0	0	0
Yellow Stingray	***Urobatis jamaicensis***	5 / 2.8	0	0	3 / 1.7 / 100	0	0	2 / 1.1 / 100
MORAY EELS	**MURAENIDAE**							
Goldentail Moray	***Gymnothorax miliaris***	1 / 0.5	0	0	1 / 0.5 / 100	0	0	0
Spotted Moray	*Gymnothorax moringa*	3 / 2.8	0	2 / 2 / 100	0	1 / 0.8 / 100	0	0
LIZARDFISHES	**SYNODONTIDAE**							
Inshore Lizardfish	***Synodus foetens***	2 / 2	0	0	0	0	2 / 2 / 100	0
Sand Diver	*Synodus intermedius*	3 / 2.7	2 / 1.7 / 100	0	0	0	1 / 1 / 100	0
FLYINGFISHES	**EXOCOETIDAE**							
Ballyhoo	*Hemiramphus brasiliensis*	900 / 563.2	0	0	0	200 / 165 / 29.2	0	700 / 398.2 / 70.7
TRUMPETFISHES	**AULOSTOMIDAE**							
Trumpetfish	*Aulostomus maculatus*	21 / 16	4 / 3.4 / 33.4	5 / 5 / 49.2	3 / 1.7 / 17.3	3 / 2.4 / 42	0	6 / 3.4 / 57.9
SCORPIONFISHES	**SCORPAENIDAE**							
Red Lionfish	***Pterois volitans***	1 / 1	0	1 / 1 / 100	0	0	0	0
Spotted Scorpionfish	*Scorpaena plumieri*	20 / 15	4 / 3.4 / 32.3	3 / 3 / 28.5	7 / 4.1 / 39	1 / 0.8 / 18.2	2 / 2 / 44.1	3 / 1.7 / 37.6
SEA BASSES	**SERRANIDAE**							
Graysby	*Cephalopholis cruentata*	110 / 84.3	19 / 16.1 / 45.7	8 / 8 / 22.6	19 / 11.1 / 31.5	19 / 15.6 / 31.9	18 / 18 / 36.7	27 / 15.3 / 31.3
Coney	*Cephalopholis fulvus*	11 / 7.4	0	0	1 / 0.5 / 100	3 / 2.4 / 35.9	1 / 1 / 14.5	6 / 3.4 / 49.5
Rock Hind	***Epinephelus adscensionis***	1 / 0.8	0	0	0	1 / 0.8 / 100	0	0

Table 3 (continued)

Species List			Transects			Point Counts		
Common Name	**Scientific Name**	**Total**	**AC**	**DC**	**OFF**	**AC**	**DC**	**OFF**
Butter Hamlet	*Hypoplectrus unicolor*	89 / 66.6	11 / 9.3 / 32.1	8 / 8 / 27.5	20 / 11.7 / 40.3	17 / 14 / 37.3	11 / 11 / 29.3	22 / 12.5 / 33.3
Orangeback Bass	***Serranus annularis***	1 / 0.5	0	0	1 / 0.5 / 100	0	0	0
Lantern Bass	*Serranus baldwini*	14 / 10.7	5 / 4.2 / 39.4	3 / 3 / 27.8	6 / 3.5 / 32.6	0	0	0
Tobaccofish	***Serranus tabacarius***	1 / 0.8	1 / 0.8 / 100	0	0	0	0	0
Harlequin Bass	*Serranus tigrinus*	93 / 73.3	15 / 12.7 / 34.3	15 / 15 / 40.3	16 / 9.3 / 25.2	15 / 12.3 / 34.1	13 / 13 / 35.9	19 / 10.8 / 29.8
JAWFISHES	**OPISTOGNATHIDAE**							
Yellowhead Jawfish	*Opistognathus aurifrons*	5 / 4.1	0	3 / 3 / 71.9	2 / 1.1 / 28	0	0	0
Dusky Jawfish	***Opistognathus whitehursti***	4 / 3.4	4 / 3.4 / 100	0	0	0	0	0
CARDINALFISHES	**APOGONIDAE**							
Flamefish	***Apogon maculatus***	1 / 0.8	0	0	0	1 / 0.8 / 100	0	0
Dusky Cardinalfish	***Phaeoptyx pigmentaria***	4 / 3.3	0	0	0	4 / 3.3 / 100	0	0
TILEFISHES	**MALACANTHIDAE**							
Sand Tilefish	*Malacanthus plumieri*	2 / 1.4	1 / 0.8 / 59.1	0	1 / 0.5 / 40.8	0	0	0
REMORAS	**ECHENEIDAE**							
Sharksucker	***Echeneis naucrates***	1 / 1	0	0	0	0	1 / 1 / 100	0
JACKS	**CARANGIDAE**							
Yellow Jack	*Carangoides bartholomaei*	22 / 17.6	3 / 2.5 / 46.5	0	5 / 2.9 / 53.4	8 / 6.6 / 54.2	5 / 5 / 41	1 / 0.5 / 4.6
Blue Runner	*Caranx crysos*	5054 / 3076.8	173 / 147 / 22.6	0	855 / 501.2 / 77.3	256 / 211.2 / 8.6	168 / 168 / 6.9	3602 / 2049.4 / 84.3
Bar Jack	*Caranx ruber*	871 / 691.3	80 / 68 / 44.2	84 / 84 / 54.6	3 / 1.7 / 1.1	111 / 91.5 / 17	252 / 252 / 46.8	341 / 194 / 36
Mackerel Scad	*Decapterus macarellus*	50 / 33.5	0	0	0	20 / 16.5 / 49.1	0	30 / 17 / 50.8
Round Scad	*Decapterus punctatus*	20 / 16.6	0	0	0	12 / 9.9 / 59.6	5 / 5 / 30.1	3 / 1.7 / 10.2
Rainbow Runner	*Elagatis bipinnulata*	34 / 20.3	0	0	0	4 / 3.3 / 16.2	0	30 / 17 / 83.7
Greater Amberjack	***Seriola dumerili***	1 / 0.8	0	0	0	1 / 0.8 / 100	0	0
Almaco Jack	***Seriola rivoliana***	1 / 0.8	0	0	0	1 / 0.8 / 100	0	0
SNAPPERS	**LUTJANIDAE**							
Mutton Snapper	*Lutjanus analis*	4 / 2.9	0	1 / 1 / 100	0	1 / 0.8 / 42	0	2 / 1.1 / 57.9

Table 3 (continued)

Species List			Transects			Point Counts		
Common Name	**Scientific Name**	**Total**	**AC**	**DC**	**OFF**	**AC**	**DC**	**OFF**
Gray Snapper	*Lutjanus griseus*	37 / 24.6	8 / 6.8 / 62.3	0	7 / 4.1 / 37.6	3 / 2.4 / 18	1 / 1 / 7.2	18 / 10.2 / 74.6
Lane Snapper	***Lutjanus synagris***	30 / 17.5	0	0	30 / 17.5 / 100	0	0	0
Yellowtail Snapper	*Ocyurus chrysurus*	821 / 578.2	31 / 26.3 / 24.9	19 / 19 / 17.9	103 / 60.3 / 57.1	137 / 113 / 23.9	133 / 133 / 28.1	398 / 226.4 / 47.9
GRUNTS	**HAEMULIDAE**							
Black Margate	*Anisotremus surinamensis*	4 / 2.7	0	0	1 / 0.5 / 100	0	1 / 1 / 46.7	2 / 1.1 / 53.2
Porkfish	*Anisotremus virginicus*	381 / 285.2	24 / 20.4 / 32.6	8 / 8 / 12.8	58 / 34 / 54.4	62 / 51.1 / 22.9	96 / 96 / 43	133 / 75.6 / 33.9
White Margate	***Haemulon album***	1 / 0.8	1 / 0.8 / 100	0	0	0	0	0
Tomtate	*Haemulon aurolineatum*	128 / 118	16 / 13.6 / 100	0	0	36 / 29.7 / 28.4	73 / 73 / 69.9	3 / 1.7 / 1.6
Caesar Grunt	*Haemulon carbonarium*	638 / 483.7	81 / 68.8 / 34.2	70 / 70 / 34.8	106 / 62.1 / 30.9	113 / 93.2 / 32.9	86 / 86 / 30.4	182 / 103.5 / 36.6
Smallmouth Grunt	*Haemulon chrysargyreum*	10 / 5.9	0	0	0	1 / 0.8 / 13.8	0	9 / 5.1 / 86.1
French Grunt	*Haemulon flavolineatum*	2735 / 2107	237 / 201.4 / 32.6	198 / 198 / 32.1	370 / 216.8 / 35.1	717 / 591.5 / 39.6	485 / 485 / 32.5	728 / 414.2 / 27.7
Spanish Grunt	***Haemulon macrostomum***	2 / 2	0	1 / 1 / 100	0	0	1 / 1 / 100	0
Sailor's Choice	*Haemulon parra*	2 / 1.3	0	0	0	1 / 0.8 / 59.1	0	1 / 0.5 / 40.8
White Grunt	*Haemulon plumierii*	252 / 190.5	31 / 26.3 / 31.2	28 / 28 / 33.2	51 / 29.8 / 35.4	54 / 44.5 / 41.9	27 / 27 / 25.4	61 / 34.7 / 32.6
Bluestriped Grunt	*Haemulon sciurus*	142 / 105.4	4 / 3.4 / 17.2	4 / 4 / 20.2	21 / 12.3 / 62.4	45 / 37.1 / 43.3	23 / 23 / 26.8	45 / 25.6 / 29.8
Juvenile Grunts	*Haemulon* spp.	440 / 326.9	53 / 45 / 60.6	11 / 11 / 14.8	31 / 18.1 / 24.4	52 / 42.9 / 16.9	100 / 100 / 39.5	193 / 109.8 / 43.4
PORGIES	**SPARIDAE**							
Jolthead Porgy	***Calamus bajonado***	6 / 3.4	0	0	2 / 1.1 / 100	0	0	4 / 2.2 / 100
Saucereye Porgy	*Calamus calamus*	6 / 5	1 / 0.8 / 34.8	1 / 1 / 41	1 / 0.5 / 24	0	2 / 2 / 77.8	1 / 0.5 / 22.1
Sheepshead Porgy	*Calamus penna*	13 / 7.8	0	1 / 1 / 100	0	0	0	12 / 6.8 / 100
Silver Porgy	*Diplodus argenteus*	9 / 7.7	0	0	0	7 / 5.7 / 74.2	2 / 2 / 25.7	0
DRUMS	**SCIAENIDAE**							
Jackknife	***Equetus lanceolatus***	1 / 0.8	0	0	0	1 / 0.8 / 100	0	0
Spotted Drum	***Equetus punctatus***	1 / 0.5	0	0	0	0	0	1 / 0.5 / 100
Cubbyu	***Equetus umbrosus***	1 / 0.5	0	0	1 / 0.5 / 100	0	0	0
Highhat	*Pareques acuminatus*	40 / 31.6	7 / 5.9 / 65.2	2 / 2 / 21.9	2 / 1.1 / 12.8	15 / 12.3 / 55	5 / 5 / 22.2	9 / 5.1 / 22.7

Table 3 (continued)

Species List			Transects			Point Counts		
Common Name	**Scientific Name**	**Total**	**AC**	**DC**	**OFF**	**AC**	**DC**	**OFF**
GOATFISHES	**MULLIDAE**							
Spotted Goatfish	*Pseudupeneus maculatus*	175 / 126.6	18 / 15.3 / 32.9	10 / 10 / 21.5	36 / 21.1 / 45.4	40 / 33 / 41	16 / 16 / 19.9	55 / 31.2 / 38.9
SEA CHUBS	**KYPHOSIDAE**							
Bermuda Sea Chub	*Kyphosus sectatrix*	317 / 223.4	1 / 0.8 / 2	6 / 6 / 14.4	59 / 34.5 / 83.4	84 / 69.3 / 38	41 / 41 / 22.5	126 / 71.6 / 39.3
BUTTERFLYFISHES	**CHAETODONTIDAE**							
Foureye Butterflyfish	*Chaetodon capistratus*	150 / 114.5	13 / 11 / 34.3	10 / 10 / 31	19 / 11.1 / 34.6	31 / 25.5 / 31	30 / 30 / 36.4	47 / 26.7 / 32.4
Spotfin Butterflyfish	*Chaetodon ocellatus*	69 / 49.8	4 / 3.4 / 22	5 / 5 / 32.3	12 / 7 / 45.5	16 / 13.2 / 38.3	7 / 7 / 20.3	25 / 14.2 / 41.3
Reef Butterflyfish	*Chaetodon sedentarius*	232 / 177.6	27 / 22.9 / 35.1	20 / 20 / 30.6	38 / 22.2 / 34.1	45 / 37.1 / 33	40 / 40 / 35.5	62 / 35.2 / 31.3
Banded Butterflyfish	*Chaetodon striatus*	31 / 22.7	1 / 0.8 / 12.6	0	10 / 5.8 / 87.3	8 / 6.6 / 41.2	6 / 6 / 37.4	6 / 3.4 / 21.3
ANGELFISHES	**POMACANTHIDAE**							
Blue Angelfish	*Holacanthus bermudensis*	62 / 48.5	6 / 5.1 / 30.3	7 / 7 / 41.6	8 / 4.6 / 27.9	11 / 9 / 28.5	13 / 13 / 40.9	17 / 9.6 / 30.4
Queen Angelfish	*Holacanthus ciliaris*	27 / 20.2	5 / 4.2 / 43.5	2 / 2 / 20.4	6 / 3.5 / 36	3 / 2.4 / 23.6	4 / 4 / 38.2	7 / 3.9 / 38
Townsend Angelfish	*Holacanthus townsendi*	2 / 1.4	0	0	1 / 0.5 / 100	1 / 0.8 / 100	0	0
Rock Beauty	*Holacanthus tricolor*	84 / 63.4	8 / 6.8 / 27.6	9 / 9 / 36.5	15 / 8.7 / 35.7	16 / 13.2 / 33.9	12 / 12 / 30.8	24 / 13.6 / 35.1
Gray Angelfish	*Pomacanthus arcuatus*	87 / 61.7	6 / 5.1 / 31.9	5 / 5 / 31.3	10 / 5.8 / 36.7	17 / 14 / 30.6	9 / 9 / 19.6	40 / 22.7 / 49.7
French Angelfish	*Pomacanthus paru*	67 / 48.5	5 / 4.2 / 26.4	3 / 3 / 18.6	15 / 8.7 / 54.8	14 / 11.5 / 35.5	9 / 9 / 27.6	21 / 11.9 / 36.7
DAMSELFISHES	**POMACENTRIDAE**							
Sergeant Major	*Abudefduf saxatilis*	664 / 497.1	47 / 39.9 / 28.8	45 / 45 / 32.5	91 / 53.3 / 38.5	166 / 136.9 / 38.1	99 / 99 / 27.5	216 / 122.8 / 34.2
Blue Chromis	*Chromis cyanea*	619 / 456.8	52 / 44.2 / 25.8	68 / 68 / 39.8	100 / 58.6 / 34.3	138 / 113.8 / 39.7	55 / 55 / 19.2	206 / 117.2 / 40.9
Yellowtail Reeffish	***Chromis enchrysura***	2 / 1.1	0	0	1 / 0.5 / 100	0	0	1 / 0.5 / 100
Sunshinefish	*Chromis insolata*	522 / 400.4	42 / 35.7 / 28.8	50 / 50 / 40.3	65 / 38.1 / 30.7	138 / 113.8 / 41.1	78 / 78 / 28.1	149 / 84.7 / 30.6
Brown Chromis	*Chromis multilineata*	582 / 440.4	30 / 25.5 / 27	29 / 29 / 30.7	68 / 39.8 / 42.2	157 / 129.5 / 37.4	109 / 109 / 31.4	189 / 107.5 / 31
Purple Reeffish	*Chromis scotti*	228 / 180.9	13 / 11 / 17.8	32 / 32 / 51.7	32 / 18.7 / 30.3	54 / 44.5 / 37.3	45 / 45 / 37.7	52 / 29.5 / 24.8
Yellowtail Damselfish	*Microspathodon chrysurus*	6 / 4.3	3 / 2.5 / 59.1	0	3 / 1.7 / 40.8	0	0	0
Dusky Damselfish	*Stegastes adustus*	188 / 147.2	31 / 26.3 / 38.6	23 / 23 / 33.7	32 / 18.7 / 27.5	42 / 34.6 / 43.7	24 / 24 / 30.3	36 / 20.4 / 25.8
Longfin Damselfish	*Stegastes diencaeus*	35 / 25.9	10 / 8.5 / 41.8	3 / 3 / 14.7	15 / 8.7 / 43.3	3 / 2.4 / 44	2 / 2 / 35.6	2 / 1.1 / 20.2

Table 3 (continued)

Species List			Transects			Point Counts		
Common Name	**Scientific Name**	**Total**	**AC**	**DC**	**OFF**	**AC**	**DC**	**OFF**
Beaugregory	*Stegastes leucostictus*	220 / 172.6	39 / 33.1 / 32.6	45 / 45 / 44.2	40 / 23.4 / 23	34 / 28 / 39.4	18 / 18 / 25.3	44 / 25 / 35.2
Bicolor Damselfish	*Stegastes partitus*	5624 / 4236.3	495 / 420.7 / 34.2	304 / 304 / 24.7	857 / 502.3 / 40.9	1543 / 1272.9 / 42.3	827 / 827 / 27.4	1598 / 909.2 / 30.2
Threespot Damselfish	*Stegastes planifrons*	17 / 14.4	7 / 5.9 / 69.7	2 / 2 / 23.4	1 / 0.5 / 6.8	1 / 0.8 / 13.8	4 / 4 / 67	2 / 1.1 / 19
Cocoa Damslefish	*Stegastes variabilis*	476 / 351.8	64 / 54.4 / 29.9	56 / 56 / 30.7	122 / 71.5 / 39.3	58 / 47.8 / 28.1	51 / 51 / 30	125 / 71.1 / 41.8
WRASSES	**LABRIDAE**							
Spotfin Hogfish	***Bodianus pulchellus***	3 / 3	0	0	0	0	3 / 3 / 100	0
Spanish Hogfish	*Bodianus rufus*	75 / 60.7	7 / 5.9 / 28.2	11 / 11 / 52.2	7 / 4.1 / 19.4	22 / 18.1 / 45.7	13 / 13 / 32.7	15 / 8.5 / 21.5
Creole Wrasse	*Clepticus parrae*	1316 / 1115.1	70 / 59.5 / 19.4	191 / 191 / 62.3	95 / 55.6 / 18.1	240 / 198 / 24.4	467 / 467 / 57.7	253 / 143.9 / 17.7
Slippery Dick	*Halichoeres bivittatus*	863 / 634.7	127 / 107.9 / 33.1	85 / 85 / 26	227 / 133 / 40.8	129 / 106.4 / 34.4	80 / 80 / 25.9	215 / 122.3 / 39.6
Yellowcheek Wrasse	*Halichoeres cyanocephalus*	27 / 19.5	6 / 5.1 / 57.5	2 / 2 / 22.5	3 / 1.7 / 19.8	3 / 2.4 / 23	2 / 2 / 18.6	11 / 6.2 / 58.3
Yellowhead Wrasse	*Halichoeres garnoti*	1412 / 1114.7	304 / 258.4 / 40.3	222 / 222 / 34.6	274 / 160.6 / 25	258 / 212.8 / 44.9	138 / 138 / 29.1	216 / 122.8 / 25.9
Clown Wrasse	*Halichoeres maculipinna*	1247 / 938.7	173 / 147 / 33.4	132 / 132 / 29.9	275 / 161.2 / 36.6	165 / 136.1 / 27.3	178 / 178 / 35.7	324 / 184.3 / 36.9
Rainbow Wrasse	*Halichoeres pictus*	51 / 41.2	0	0	0	14 / 11.5 / 28	20 / 20 / 48.5	17 / 9.6 / 23.4
Blackear Wrasse	*Halichoeres poeyi*	50 / 36.7	10 / 8.5 / 31.1	10 / 10 / 36.6	15 / 8.7 / 32.2	2 / 1.6 / 17.4	1 / 1 / 10.5	12 / 6.8 / 72
Puddingwife	*Halichoeres radiatus*	50 / 35.6	3 / 2.5 / 20.9	2 / 2 / 16.4	13 / 7.6 / 62.6	9 / 7.4 / 31.5	7 / 7 / 29.7	16 / 9.1 / 38.6
Hogfish	*Lachnolaimus maximus*	42 / 28	2 / 1.7 / 7.6	3 / 3 / 13.4	30 / 17.5 / 78.9	2 / 1.6 / 28.5	3 / 3 / 51.8	2 / 1.1 / 19.6
Bluehead Wrasse	*Thalassoma bifasciatum*	6620 / 4947.8	714 / 606.9 / 29.5	690 / 690 / 33.5	1294 / 758.5 / 36.9	1339 / 1104.6 / 38.1	738 / 738 / 25.5	1845 / 1049.7 / 36.2
Green Razorfish	*Xyrichtys splendens*	8 / 6.8	2 / 1.7 / 24.7	4 / 4 / 58.2	2 / 1.1 / 17	0	0	0
PARROTFISHES	**SCARIDAE**							
Bluelip Parrotfish	*Cryptotomus roseus*	333 / 248.9	65 / 55.2 / 43.6	35 / 35 / 27.6	62 / 36.3 / 28.7	61 / 50.3 / 41.1	22 / 22 / 17.9	88 / 50 / 40.9
Parrotfish species	*Scaridae* spp.	1 / 0.5	0	0	0	0	0	1 / 0.5 / 100
Midnight Parrotfish	*Scarus coelestinus*	3 / 2.1	0	0	1 / 0.5 / 100	0	1 / 1 / 63.7	1 / 0.5 / 36.2
Blue Parrotfish	*Scarus coeruleus*	4 / 3.6	1 / 0.8 / 45.9	1 / 1 / 54	0	1 / 0.8 / 45.2	1 / 1 / 54.7	0
Rainbow Parrotfish	*Scarus guacamaia*	14 / 8.9	0	1 / 1 / 100	0	2 / 1.6 / 20.8	0	11 / 6.2 / 79.1
Striped Parrotfish	*Scarus iseri*	800 / 615	106 / 90.1 / 30.4	113 / 113 / 38.2	158 / 92.6 / 31.3	137 / 113 / 35.3	101 / 101 / 31.6	185 / 105.2 / 32.9

Table 3 (continued)

Species List			Transects			Point Counts		
Common Name	**Scientific Name**	**Total**	**AC**	**DC**	**OFF**	**AC**	**DC**	**OFF**
Princess Parrotfish	*Scarus taeniopterus*	572 / 414	48 / 40.8 / 24.6	47 / 47 / 28.3	133 / 77.9 / 47	96 / 79.2 / 31.8	65 / 65 / 26.1	183 / 104.1 / 41.9
Queen Parrotfish	*Scarus vetula*	63 / 47.1	3 / 2.5 / 53.9	1 / 1 / 21.1	2 / 1.1 / 24.8	19 / 15.6 / 36.9	12 / 12 / 28.2	26 / 14.7 / 34.8
Greenblotch Parrotfish	*Sparisoma atomarium*	447 / 339.9	67 / 56.9 / 29.6	63 / 63 / 32.8	123 / 72.1 / 37.5	64 / 52.8 / 35.7	49 / 49 / 33.1	81 / 46 / 31.1
Redband Parrotfish	*Sparisoma aurofrenatum*	2182 / 1662.3	304 / 258.4 / 35.9	234 / 234 / 32.5	386 / 226.2 / 31.4	397 / 327.5 / 34.7	293 / 293 / 31	568 / 323.1 / 34.2
Redtail Parrotfish	*Sparisoma chrysopterum*	87 / 66.6	2 / 1.7 / 25.6	2 / 2 / 30.1	5 / 2.9 / 44.2	29 / 23.9 / 39.8	19 / 19 / 31.6	30 / 17 / 28.4
Bucktooth Parrotfish	*Sparisoma radians*	253 / 194.7	40 / 34 / 29.2	36 / 36 / 30.9	79 / 46.3 / 39.8	48 / 39.6 / 50.5	24 / 24 / 30.6	26 / 14.7 / 18.8
Redfin Parrotfish	*Sparisoma rubripinne*	48 / 38.4	1 / 0.8 / 8.6	6 / 6 / 61.3	5 / 2.9 / 29.9	27 / 22.2 / 77.6	3 / 3 / 10.4	6 / 3.4 / 11.8
Stoplight Parrotfish	*Sparisoma viride*	309 / 234.1	47 / 39.9 / 34.2	38 / 38 / 32.5	66 / 38.6 / 33.1	39 / 32.1 / 27.3	41 / 41 / 34.8	78 / 44.3 / 37.7
COMBTOOTH BLENNIES	**BLENNIDAE**							
Barred Blenny	*Hypleurochilus bermudensis*	2 / 1.5	0	1 / 1 / 63	1 / 0.5 / 36.9	0	0	0
Redlip Blenny	*Ophioblennius macclurei*	2 / 1.3	0	0	0	1 / 0.8 / 59.1	0	1 / 0.5 / 40.8
Seaweed Blenny	*Parablennius marmoreus*	79 / 60.8	18 / 15.3 / 36.1	10 / 10 / 23.6	29 / 17 / 40.1	10 / 8.2 / 44.5	8 / 8 / 43.1	4 / 2.2 / 12.2
CLINIDS	**CLINIDAE**							
Hairy Blenny	***Labrisomus nuchipinnis***	4 / 3.4	4 / 3.4 / 100	0	0	0	0	0
Rosy Blenny	*Malacoctenus macropus*	87 / 67.3	26 / 22.1 / 40.9	16 / 16 / 29.6	27 / 15.8 / 29.3	4 / 3.3 / 24.5	5 / 5 / 37.2	9 / 5.1 / 38.1
Saddled Blenny	*Malacoctenus triangulatus*	82 / 61.7	22 / 18.7 / 39.2	12 / 12 / 25.1	29 / 17 / 35.6	6 / 4.9 / 35.1	4 / 4 / 28.4	9 / 5.1 / 36.3
Banded Blenny	***Paraclinus fasciatus***	1 / 1	0	1 / 1 / 100	0	0	0	0
TUBE BLENNIES	**CHAENOPSIDAE**							
Roughhead Blenny	*Acanthemblemaria aspera*	10 / 7.7	4 / 3.4 / 43.9	2 / 2 / 25.8	4 / 2.3 / 30.2	0	0	0
Sailfin Blenny	*Emblemaria pandionis*	5 / 4.1	0	2 / 2 / 63	2 / 1.1 / 36.9	0	1 / 1 / 100	0
GOBIES	**GOBIIDAE**							
Colon Goby	*Coryphopterus dicrus*	50 / 37.6	9 / 7.6 / 22.4	13 / 13 / 38	23 / 13.4 / 39.5	1 / 0.8 / 23.3	1 / 1 / 28.3	3 / 1.7 / 48.3
Bridled Goby	*Coryphopterus glaucofraenum*	266 / 211.5	91 / 77.3 / 44.8	53 / 53 / 30.7	72 / 42.2 / 24.4	21 / 17.3 / 44.4	12 / 12 / 30.7	17 / 9.6 / 24.8
Masked/Glass Goby	*Coryphopterus hyalinus/personatus*	14055 / 9954	1381 / 1173.8 / 20.9	1140 / 1140 / 20.3	5605 / 3285.6 / 58.6	2034 / 1678 / 38.5	1068 / 1068 / 24.5	2827 / 1608.4 / 36.9
Spotted Goby	***Coryphopterus punctipectophorus***	1 / 0.5	0	0	1 / 0.5 / 100	0	0	0

Table 3 (continued)

Species List			Transects			Point Counts		
Common Name	**Scientific Name**	**Total**	**AC**	**DC**	**OFF**	**AC**	**DC**	**OFF**
Dash Goby	*Ctenogobius saepepallens*	11 / 8.1	5 / 4.2 / 55.9	1 / 1 / 13.1	4 / 2.3 / 30.8	0	0	1 / 0.5 / 100
Neon Goby	*Elacatinus oceanops*	32 / 22.2	1 / 0.8 / 6.8	4 / 4 / 32	13 / 7.6 / 61.1	2 / 1.6 / 16.8	3 / 3 / 30.7	9 / 5.1 / 52.4
Goldspot Goby	*Gnatholepis thompsoni*	117 / 98.9	22 / 18.7 / 31.3	31 / 31 / 51.9	17 / 9.9 / 16.7	34 / 28 / 71.3	9 / 9 / 22.8	4 / 2.2 / 5.7
Code Goby	*Gobiosoma robustum*	3 / 2.8	1 / 0.8 / 29.8	2 / 2 / 70.1	0	0	0	0
Blue Goby	*Ptereleotris calliura*	3 / 2.4	1 / 0.8 / 34.8	1 / 1 / 41	1 / 0.5 / 24	0	0	0
SPADEFISHES	**EPHIPPIDAE**							
Atlantic Spadefish	*Chaetodipterus faber*	37 / 33.1	0	0	6 / 3.5 / 100	3 / 2.4 / 8.3	26 / 26 / 87.7	2 / 1.1 / 3.8
SURGEONFISHES	**ACANTHURIDAE**							
Ocean surgeon	*Acanthurus bahianus*	3157 / 2418.3	404 / 343.4 / 37.4	241 / 241 / 26.2	568 / 332.9 / 36.2	625 / 515.6 / 34.3	545 / 545 / 36.3	774 / 440.3 / 29.3
Doctorfish	*Acanthurus chirurgus*	649 / 477.9	51 / 43.3 / 22.2	59 / 59 / 30.2	158 / 92.6 / 47.5	85 / 70.1 / 24.7	103 / 103 / 36.4	193 / 109.8 / 38.8
Blue Tang	*Acanthurus coeruleus*	483 / 379.4	59 / 50.1 / 48.8	25 / 25 / 24.3	47 / 27.5 / 26.8	85 / 70.1 / 25.3	127 / 127 / 45.8	140 / 79.6 / 28.7
MACKERELS	**SCOMBRIDAE**							
Cero	*Scomberomoros regalis*	36 / 26.1	6 / 5.1 / 28.7	5 / 5 / 28.2	13 / 7.6 / 43	3 / 2.4 / 29.2	2 / 2 / 23.6	7 / 3.9 / 47
King Mackerel	***Scomberomorous cavalla***	1 / 1	0	0	0	0	1 / 1 / 100	0
TRIGGERFISHES	**BALISTIDAE**							
Gray Triggerfish	*Balistes capriscus*	23 / 16.2	3 / 2.5 / 28.1	3 / 3 / 33	6 / 3.5 / 38.7	2 / 1.6 / 22.9	1 / 1 / 13.8	8 / 4.5 / 63.2
Ocean Triggerfish	***Canthidermis sufflamen***	1 / 0.8	0	0	0	1 / 0.8 / 100	0	0
FILEFISHES	**MONACANTHIDAE**							
Unicorn Filefish	*Aluterus monoceros*	3 / 2.1	0	0	0	0	1 / 1 / 46.7	2 / 1.1 / 53.2
Orange Filefish	***Aluterus schoepfi***	2 / 1.1	0	0	0	0	0	2 / 1.1 / 100
Scrawled Filefish	*Aluterus scriptus*	79 / 61.1	2 / 1.7 / 19.3	3 / 3 / 34	7 / 4.1 / 46.6	17 / 14 / 26.7	23 / 23 / 43.9	27 / 15.3 / 29.3
Orangespotted Filefish	*Cantherhines pullus*	50 / 39.3	6 / 5.1 / 34.4	5 / 5 / 33.8	8 / 4.6 / 31.7	12 / 9.9 / 40.2	9 / 9 / 36.6	10 / 5.6 / 23.1
Fringed Filefish	*Monacanthus ciliatus*	2 / 1.4	0	0	1 / 0.5 / 100	1 / 0.8 / 100	0	0
Slender Filefish	***Monacanthus tuckeri***	1 / 1	0	0	0	0	1 / 1 / 100	0
Planehead Filefish	***Stephanolepis hispidus***	1 / 0.5	0	0	1 / 0.5 / 100	0	0	0
BOXFISHES	**OSTRACIIDAE**							

Table 3 (continued)

Species List			Transects			Point Counts		
Common Name	**Scientific Name**	**Total**	**AC**	**DC**	**OFF**	**AC**	**DC**	**OFF**
Honeycomb Cowfish	*Acanthostracion polygonius*	5 / 4.3	2 / 1.7 / 100	0	0	2 / 1.6 / 62.2	1 / 1 / 37.7	0
Scrawled Cowfish	***Acanthostracion quadricornis***	2 / 1.1	0	0	1 / 0.5 / 100	0	0	1 / 0.5 / 100
Spotted Trunkfish	*Lactophrys bicaudalis*	11 / 8.8	1 / 0.8 / 59.1	0	1 / 0.5 / 40.8	4 / 3.3 / 44.3	3 / 3 / 40.3	2 / 1.1 / 15.2
Smooth Trunkfish	*Lactophrys triqueter*	19 / 13.9	1 / 0.8 / 21.1	2 / 2 / 49.7	2 / 1.1 / 29.1	6 / 4.9 / 49.8	1 / 1 / 10	7 / 3.9 / 40
PUFFERS	**TETRAODONTIDAE**							
Sharpnose Puffer	*Canthigaster rostrata*	716 / 559.7	134 / 113.9 / 35.1	108 / 108 / 33.3	174 / 102 / 31.4	98 / 80.8 / 34.2	93 / 93 / 39.4	109 / 62 / 26.2
Bandtail Puffer	*Sphoeroides spengleri*	5 / 3.3	0	0	0	2 / 1.6 / 49.1	0	3 / 1.7 / 50.8
PORCUPINEFISHES	**DIODONTIDAE**							
Striped Burrfish	*Chilomycterus schoepfi*	9 / 8.1	0	0	0	0	7 / 7 / 86	2 / 1.1 / 13.9
Balloonfish	*Diodon holocanthus*	34 / 24.7	5 / 4.2 / 25.1	5 / 5 / 29.6	13 / 7.6 / 45.1	3 / 2.4 / 31.3	2 / 2 / 25.3	6 / 3.4 / 43.2
Porcupinefish	*Diodon hystrix*	9 / 6.4	0	0	0	2 / 1.6 / 25.4	2 / 2 / 30.7	5 / 2.8 / 43.8
	Total Abundance	**60588 / 44432.5**	**6106 / 5190.1**	**4885 / 4885**	**13482 / 7903.2**	**10715 / 8839.8**	**7354 / 7354**	**18046 / 10267.5**
	Total Species	**151**	**97**	**93**	**108**	**109**	**98**	**107**
	Mean Density (Fish/m^2 ± SEM)	**-**	**0.56 ± 0.16**	**0.53 ± 0.16**	**0.86 ± 0.38**	**0.33 ± 0.09**	**0.27 ± 0.07**	**0.38 ± 0.11**
	Total # of shaded cells	**-**	**35**	**32**	**57**	**49**	**32**	**50**

Table 4: Mean fish per count by quarter, power state, and count type (±SEM (N = 44 Shallow, 44 Middle, 44 Deep; N = 80 AC, 67 DC, 116 OFF)

	Transects			Point-counts		
	AC	**DC**	**OFF**	**AC**	**DC**	**OFF**
Quarter 1	145.3 ±43.9	n/a	218.5 ±59	239.2 ±51.3	n/a	239.2 ±34.4
Quarter 2	250.8 ±43.3	225.8 ±60.7	559.3 ±182	376.3 ±80.4	389.4 ±114.6	466.4 ±126.1
Quarter 3	160 ±31.5	166.2 ±22.2	201.4 ±32.5	343 ±70.6	284.5 ±78.5	475.1 ±127.4
Quarter 4	134.6 ±21.1	107.5 ±18.2	106.1 ±12.5	216.1 ±33.9	183.1 ±24.9	167.2 ±17.4
Quarter 5	120 ±17.2	127.8 ±22.7	130 ±15.1	233.6 ±45.2	150.3 ±12.6	212.6 ±43.8
Mean	152.9 ±13.8	144.7 ±15.7	234.9 ±43.9	281.6 ±24.6	251.8 ±27.1	312.1 ±41.7

VIII. REFERENCES

An, E., M R Dhanak, L K Shay, S Smith and J Van Leer. Coastal Oceanography using a small AUV. 2001, Journal of Atmospheric and Ocean Technology, 18, 215-234.

Banks, K.W., Riegl, B.M., Shinn, E.A., Piller, W.E., & Dodge, R.E. (2007). Geomorphology of the southeast Florida continental reef tract (Miami-Dade, Broward, and Palm Beach counties, USA). *Coral Reefs,* 26(3), 617-633.

Baron, R.M., Jordan, L.K., & Spieler, R.E. (2004). Characterization of the marine fish assemblage associated with the nearshore hardbottom of Broward County, Florida, USA. *Estuarine, Coastal and Shelf Science,* 60(3), 431-443.

Brandt, M.E., N. Zurcher, A. Acosta, J.S. Ault, J.A. Bohnsack, M.W. Feeley, D.E. Harper, J. Hunt, T. Kellison, D.B. McClellan, M.E. Patterson and S.G. Smith. 2009. A cooperative multi-agency reef fish monitoring protocol for the Florida Keys coral reef ecosystem. Natural Resource Report NPS/SFCN/NRR – 2009/150. National Park Service, Fort Collins, Colorado.

Bohnsack, J.A., & Bannerot, S.P. (1986). A stationary visual census technique for quantitatively assessing community structure of coral reef fishes. *NOAA Technical Report NMFS 41*. 15 pp.

Castro, José I. 1996. Biology of the Blacktip Shark, *Carcharhinus Limbatus*, off the Southeastern United States. Bulletin of Marine Science 59 (3): 508-522

Chagnaud, B.P., Wilkens, L.A., & Hofmann, M.H. (2008). Response properties of electrosensory neurons in the lateral mesencephalic nucleus of the paddlefish. *Journal of Comparative Physiology A*, 194(3), 209-220.

Clarke, K.R., & Warwick, R.M. (2001). An approach to statistical analysis and interpretation. *Change in Marine Communities*, 2. Plymouth Marine Laboratory, UK.

Centre for Marine and Coastal Studies (CMACS). (2003). A Baseline Assessment of Electromagnetic Fields Generated by Offshore Windfarm Cables (COWRIE Technical Report EMF 01-2002 66), Birkenhead, England, UK

Dhanak, M, Edgar An and Karl von Ellenrieder, William Venezia, Characterization of the Magnetic Field in Coastal Waters Using an AUV. 2013. Oceans/MTS conference. San Diego. September 2013.

Dhanak, M, R. Coulson, E. Henderson, J. Frankenfield, D. Pugsley, S. Ravenna, G. Valdes, W. Venezia, "AUV-Based Characterization of EMF Emissions from Submerged Power Cables", Oceans/MTS conference 2015. Genoa, Italy. May 2015.

Dhanak, M. R. and K Holappa. 1999. An Autonomous Ocean Turbulence Measurement Platform. Journal of Atmospheric and Ocean Technology, 16, 1506 - 1518

Duerr, Alana E. S. and Manhar R Dhanak. 2012. An assessment of the hydrokinetic energy resource of the Florida Current. IEEE Journal of Oceanic Engineering. Volume 37, Issue 2, pp. 281 – 293.

Ferro, F.M., Jordan, L.K., & Spieler, R.E. (2005). The marine fishes of Broward County, Florida: Final report of 1998-2002 survey results. *NOAA Technical Memorandum NMFS-SEFSC-532*, 73 pp.

Fisher, C., M. Slater. 2010. Effects of electromagnetic fields on marine species: A literature review. Report. Oregon Wave Energy Trust

Gill A.B. and H. Taylor. 2002. The Potential Effects of Electromagnetic Field Generated by Cabling between Offshore Wind Turbines upon Elasmobranch Fishes. Report to the Countryside Council for Wales (CCW Contract Science Report No 488).

Gilliam, D.S., Dodge, R.E., Spieler, R.E., Halperin, A.A., C. Walton & K. Kilfoyle. (2013). Marine Biological Monitoring in Broward County, Florida: Year 14 (2013) *Annual Report*, 121 pp.

Helfman, G. S., Collette, B. B., Facey, D. E., & Bowen, B. W. (2009). The diversity of fishes: biology, evolution and ecology. 2. Blackwell Publishing, Oxford. 720pp

Jeong, J.H., Choi, K.B., Moon, N.J., Park, E.S., & Sohn, U.D. (2005). Benzodiazepine system is involved in hyperalgesia in rats induced by the exposure to extremely low frequency magnetic fields. *Archives of Pharmacal Research*, *28*(2), 238-242.

Kilfoyle, K., Walker, B.K., Fisco, D.P., Smith, S.G., and R.E. Spieler. (2015). Southeast Florida Coral Reef Fishery-Independent Baseline Assessment – 2012-2014 *Summary Report*. Florida Department of Environmental Protection. 129 pp.

Klimley, A.P., Beavers, S.C., Curtis, T.H., Jorgensen, S.J., 2002. Movements and swimming behavior of three species of sharks in La Jolla Canyon, California. Environ. Biol. Fish. 63, 117-135.

Kirschvink, J. L., A. E. Dizon, and J. A. Westphal. "Evidence from strandings for geomagnetic sensitivity in cetaceans." *Journal of Experimental Biology* 120:1-24. 1986.

Krylov V.V., Chebotareva Y.V., & Izyumov, Y.G. (2016). Delayed consequences of extremely low-frequency magnetic fields and the influence of adverse environmental conditions on roach *Rutilus rutilus* embryos. *Journal of Fish Biology*. In Press.

Lee, D., Lee, J., & Lee, I. (2015). Cell phone-generated radio frequency electromagnetic field effects on the locomotor behaviors of the fishes *Poecilia reticulata* and *Danio rerio*. *International Journal of Radiation Biology*, 91(10), 843-850.

Lee, W., & Yang, K. L. (2014). Using medaka embryos as a model system to study biological effects of the electromagnetic fields on development and behavior. Ecotoxicology and Environmental Safety, 108, 187-194.

Lewczuk, B., Redlarski, G., Zak, A., Ziolkowska, N., Przybylska-Gornowicz, B., & Krawczuk, M. (2014). Influence of Electric, Magnetic, and Electromagnetic Fields on the Circadian System: Current Stage of Knowledge. *Biomedical Research International*, 2014, 1-13.

Lieske, E., & Myers, R. F. (2002). Coral reef fishes: Indo-pacific and Caribbean. Princeton, New Jersey: Princeton University Press.

Li, B.L., Li, W., Bi, J.Q., Zhao, J.G., Qu, Z.W., Lin, C., Yang, S.L., Meng, Q.G., & Yue Q. (2015). Effect of long-term pulsed electromagnetic field exposure on hepatic and immunologic functions of rats. *Wiener Klinische Wochenschrift*, 27: 959-962

Lucca Giovanni. Analytical Evaluation of Sub-Sea ELF Electromagnetic Field Generated by Submarine Power Cables. Progress In Electromagnetics Research B, Vol. 56, 309–326, 2013

Öhman, M.C., Sigray, P., & Westerberg, H. (2007). Offshore windmills and the effects of electromagnetic fields on fish. *AMBIO: A journal of the Human Environment*, 36(8), 630-633.

Pall, M.L. (2015). Scientific evidence contradicts findings and assumptions of Canadian Safety Panel 6: microwaves act through voltage-gated calcium channel activation to induce biological impacts at non-thermal levels, supporting a paradigm shift for microwave/lower frequency electromagnetic field action. *Reviews on Environmental Health*, *30*(2), 99-116.

Putman, N.F., Meinke, A.M., & Noakes, D.L. (2014). Rearing in a distorted magnetic field disrupts the 'map sense'of juvenile steelhead trout. *Biology Letters*, 10(6) 20140169.

Schwartz, F. J. (1990). Mass migratory congregations and movements of several species of cownose rays, genus Rhinoptera: a world-wide review. The Journal of the Elisha Mitchell Scientific Society106, 10–13.

Smith, S.G., J.S. Ault, J.A. Bohnsack, D.E. Harper, J. Luo and D.B. McClellan. 2011. Multispecies survey design for assessing reef-fish stocks, spatially-explicit management performance, and ecosystem condition. *Fisheries Research* 109: 25-41.

Spieler, R.E., D.P. Fahy, R.L. Sherman, J. Sulowkoski, T.P. Quinn. 2013. The Yellow Stingray, *Urobatis jamaicensis* (Chondrichthyes: Urotrygonidae): a synoptic review. Caribbean Journal of Science. 47(1) 67-97.

Sugishita, M., & Takayama, Y. (1993). Paraesthesia elicited by repetitive magnetic stimulation of the postcentral gyrus. *Neuroreport*, *4*(5), 569-570.

Tabor, K.M., Bergeron, S.A., Horstick, E.J., Jordan, D.C., Aho, V., Porkka-Heiskanen, T., Haspel, G. & Burgess, H.A. (2014). Direct activation of the Mauthner cell by electric field pulses drives ultrarapid escape responses. *Journal of Neurophysiology*, *112*(4), 834-844.

Tricas, Timothy and Andrew Gill 'Effects of EMFs from Undersea Power Cables on Elasmobranchs and Other Marine Species.' 2011. Final Report. U.S. Department of the Interior. Bureau of Ocean Energy Management, Regulation, and Enforcement.

Varanelli, C.C., & J.D. McCleave. (1974). Locomotor activity of Atlantic salmon parr (Salmo salar L.) in various light conditions and in weak magnetic fields. *Animal Behavior*, 22: 178-186.

Varró, P., Szemerszky, R., Bárdos, G., & Világi, I. (2009). Changes in synaptic efficacy and seizure susceptibility in rat brain slices following extremely low-frequency electromagnetic field exposure. *Bioelectromagnetics*, *30*(8), 631-640.

Venezia, W, W. Baxley, P. Tatro, M. Dhanak, F.R. Driscoll, P. Beaujean, S. Shock,S. Glegg, E. An, M. Luther, B. Weisberg, H. DeFerrari, N. Williams, H. Nguyen, N.Shay, J. Van Leer, R. Dodge, D. Gilliam, A. Soloviev, S. Pomponi, M. Crane, and K.Carter. SFOMC, A Successful Navy And Academic Partnership Providing Sustained Ocean Observation Capabilities in the Florida Straits, 2003, Marine Technology Society Journal, Vol. 37, 81-91

Wang, Z., Wang, L., Zheng, S., Ding, Z., Liu, H., Jin, W., Pan, Y., Chen, Z., Fei., Y, Chen, G., Xu, Z. & Xu, Z. (2016). Effects of electromagnetic fields on serum lipids in workers of a power plant. *Environmental Science and Pollution Research*, *23*(3), 2495-2504.

Ward, B.K., Tan, G.X., Roberts, D.C., Della Santina, C.C., Zee, D.S., & Carey, J.P. (2014). Strong static magnetic fields elicit swimming behaviors consistent with direct vestibular stimulation in adult zebrafish. *PLOS ONE 9(3): e92109. doi: 10.1371/journal.pone.0092109*

Westerberg, H., and I. Lagenfelt, 2008, Sub-sea power cables and the migration behaviour of the European eel. Fisheries Management and Ecology, Volume 15, Issue 5-6, pages 369–375

IX. PRODUCTS / DELIVERABLES

This final report is due at this time.

Following publications have resulted from the effort:

- *AUV-Based Characterization of EMF Emissions from Submerged Power Cables.* Manhar Dhanak et al. 2015. MTS/IEEE Oceans Conference, Genoa, Italy, May 2015.
- *Characterization of EMF Emissions from Submarine Cables and Monitoring for Potential Responses of Marine Species.* Dhanak, M., Kilfoyle, A., Ravenna, S., Coulson, R., Frankenfield, J., Jermain, R., Valdes, G., Spieler, R. 11th European Wave and Tidal Energy Conference. Nantes, France, September 2015.
- *Assessment of Electromagnetic Field Emissions from Subsea Cables*. Dhanak, M., R. Coulson, C. Dibiasio, J. Frankenfield, E. Henderson, D. Pugsley, G. Valdes. 2016 NHA METS Poster, Washington, DC, April, 2016.
- *Effects of EMF Emissions from Undersea Electric Cables on Coral Reef Fishes*. Kilfoyle, A., R. Jermain, M. Dhanak, J. Huston, R. Spieler. Submitted to Bioelectromagnetics.

Database: A database of EMF measurement and observed potential organismal responses, including, raw data, figures, tables, photos and videos, has been prepared. Depositories such as MHKDR and Tethys are being considered for archiving the data.

Patents: N/A

X. IMPACT

The project makes impact on the following:

- Development of procedures and sensor to measure E-M fields in the water column over power-transmitting cables using an AUV.
- Coordination of personnel and assets to concurrently collect video (from air and underwater), EMF measurements, and SCUBA diver-based observations for aquatic species responses to power transmitting cables in both power on and power off conditions.
- Development of procedures to collect video over power-transmitting cables from fixed seafloor stations and moving AUV platforms.
- Development of a database of project-specific data to characterize EMF emissions effects from power transmitting cables on marine species.

XI. PARTICIPANTS & OTHER COLLABORATING ORGANIZATIONS

A. Individuals:

Name	Dr. Manhar Dhanak
Project Role	PI
Nearest Person Month worked	1 month
Contribution to Project	Overall Project coordination and supervision;
Funding Support	
Collaborated w/ individual in foreign country	No
Country(ies) of foreign collaborator	N/A
Traveled to foreign country	No
If traveled to foreign country, duration of stay	N/A

Name	John Frankenfield
Project Role	Staff Engineer
Nearest Person Month worked	1 months
Contribution to Project	Mr. Frankenfield has participated in planning and preparing the AUV, AUV cameras, underwater video stations, independent lab test water tank, offshore operations, and general engineering and machining.
Funding Support	
Collaborated w/ individual in foreign country	No
Country(ies) of foreign collaborator	N/A
Traveled to foreign country	No
If traveled to foreign country, duration of stay	N/A

Name	Christopher Dibiasio
Project Role	MS graduate student
Nearest Person Month worked	1.5 months
Contribution to Project	Mr. Dibiasio has prepared the magnetometer for EMF surveys and supported offshore AUV tests
Funding Support	

Collaborated w/ individual in foreign country	No
Country(ies) of foreign collaborator	N/A
Traveled to foreign country	No
If traveled to foreign country, duration of stay	N/A

Name	Robert Coulson
Project Role	Staff Engineer
Nearest Person Month worked	1 month
Contribution to Project	Mr. Coulson participated in planning and preparing the AUV, the design of the Electric field sensor, offshore operations, and general engineering
Funding Support	
Collaborated w/ individual in foreign country	No
Country(ies) of foreign collaborator	N/A
Traveled to foreign country	No
If traveled to foreign country, duration of stay	N/A

Name	Edward Henderson
Project Role	Staff Engineer
Nearest Person Month worked	3 months
Contribution to Project	Mr. Henderson led the integrated design, construction, and testing of the Electric field sensor.
Funding Support	
Collaborated w/ individual in foreign country	No
Country(ies) of foreign collaborator	N/A
Traveled to foreign country	No
If traveled to foreign country, duration of stay	N/A

Name	Shirley Ravenna
Project Role	Staff Engineer
Nearest Person Month worked	1.5 months

Contribution to Project	Ms. Ravenna participated in project planning documentation, offshore operations, and general engineering
Funding Support	
Collaborated w/ individual in foreign country	No
Country(ies) of foreign collaborator	N/A
Traveled to foreign country	No
If traveled to foreign country, duration of stay	N/A

Name	Richard Spieler
Project Role	Co-PI
Nearest Person Month worked	1 month
Contribution to Project	NSU Project coordination and supervision
Funding Support	
Collaborated w/ individual in foreign country	No
Country(ies) of foreign collaborator	N/A
Traveled to foreign country	No
If traveled to foreign country, duration of stay	N/A

Name	Kirk Kilfoyle
Project Role	PhD student – project coordinator
Nearest Person Month worked	1 month
Contribution to Project	Site selection, site preparation, logistical and diving support, coordination and meetings with FAU and Navy personnel as needed, analysis and preparation of SCUBA survey data.
Funding Support	
Collaborated w/ individual in foreign country	No
Country(ies) of foreign collaborator	N/A
Traveled to foreign country	No
If traveled to foreign country, duration of stay	N/A

Name	Robert Jermain
Project Role	MS graduate student
Nearest Person Month worked	1.5 months
Contribution to Project	Site selection, site preparation, surveys, data entry, coordination with FAU and Navy personnel as needed. Assisted with preparations for independent laboratory testing tank.
Funding Support	
Collaborated w/ individual in foreign country	No
Country(ies) of foreign collaborator	N/A
Traveled to foreign country	No
If traveled to foreign country, duration of stay	N/A

Name	Dana Fisco
Project Role	MS graduate student
Nearest Person Month worked	1 month
Contribution to Project	Field and diving support
Funding Support	
Collaborated w/ individual in foreign country	No
Country(ies) of foreign collaborator	N/A
Traveled to foreign country	No
If traveled to foreign country, duration of stay	N/A

Name	Allison Patranella
Project Role	MS graduate student
Nearest Person Month worked	1 month
Contribution to Project	Field and diving support
Funding Support	
Collaborated w/ individual in foreign country	No
Country(ies) of foreign collaborator	N/A
Traveled to foreign country	No
If traveled to foreign country, duration of stay	N/A

Name	Morgan Knowles
Project Role	MS graduate student
Nearest Person Month worked	1 month
Contribution to Project	Field and diving support
Funding Support	
Collaborated w/ individual in foreign country	No
Country(ies) of foreign collaborator	N/A
Traveled to foreign country	No
If traveled to foreign country, duration of stay	N/A

B. Organizations:

Florida Atlantic University

SeaTech, 101 North Beach Road,

Dania Beach, FL 33004.

FAU leads the project and coordinates the collaboration between the partnering organizations. FAU is responsible for characterizing EMF levels at the survey sites. FAU is also responsible for collecting AUV-based video of marine-species responses in complement to the SCUBA diver surveys, establishing fixed video monitoring stations at selected locations, and conducting synoptic aerial surveys.

Nova Southeastern University Oceanographic Center

8000 North Ocean Drive

Dania Beach, FL 33004

NSU provides diving support in terms of facilities and personnel as well as marine biology expertise, essential for identifying proper in-water surveying sites, implementing standard surveying methods, and characterizing aquatic species and responses.

South Florida Ocean Measurement Facility

Naval Surface Warfare Center, Carderock Division

91 North Beach Rd.

Dania Beach, FL 33004

SFOMF provides the offshore facility containing the project designated submarine cable and fixed electromagnetic measurement arrays assets on the seafloor, as well as personnel to control and monitor the aforementioned assets.